Full-length Article

Dietary fatty acid composition drives neuroinflammation and impaired behavior in obesity

Clara Sanchez [a], Cécilia Colson [a,b], Nadine Gautier [b], Pascal Noser [c], Juliette Salvi [d], Maxime Villet [a], Lucile Fleuriot [a], Caroline Peltier [d], Pascal Schlich [d], Frédéric Brau [a], Ariane Sharif [e], Ali Altintas [c], Ez-Zoubir Amri [b], Jean-Louis Nahon [a], Nicolas Blondeau [a], Alexandre Benani [d], Romain Barrès [a,c], Carole Rovère [a,*]

[a] Université Côte d'Azur, Institut de Pharmacologie Moléculaire et Cellulaire, CNRS, France
[b] Université Côte d'Azur, Institut de Biologie de Valrose, CNRS, INSERM, France
[c] Novo Nordisk Foundation Center for Basic Metabolic Research, University of Copenhagen, Denmark
[d] Université Bourgogne Franche-Comté, Centre des Sciences du Goût et de l'Alimentation, CNRS, INRAe, France
[e] Université de Lille, CHU Lille, Laboratory of Development and Plasticity of the Neuroendocrine Brain, Lille Neurosciences & Cognition, UMR-S 1172, Lille France

ARTICLE INFO

ABSTRACT

Nutrient composition in obesogenic diets may influence the severity of disorders associated with obesity such as insulin-resistance and chronic inflammation. Here we hypothesized that obesogenic diets rich in fat and varying in fatty acid composition, particularly in omega 6 (ω6) to omega 3 (ω3) ratio, have various effects on energy metabolism, neuroinflammation and behavior. Mice were fed either a control diet or a high fat diet (HFD) containing either low (LO), medium (ME) or high (HI) ω6/ω3 ratio. Mice from the HFD-LO group consumed less calories and exhibited less body weight gain compared to other HFD groups. Both HFD-ME and HFD-HI impaired glucose metabolism while HFD-LO partly prevented insulin intolerance and was associated with normal leptin levels despite higher subcutaneous and perigonadal adiposity. Only HFD-HI increased anxiety and impaired spatial memory, together with increased inflammation in the hypothalamus and hippocampus. Our results show that impaired glucose metabolism and neuroinflammation are uncoupled, and support that diets with a high ω6/ω3 ratio are associated with neuroinflammation and the behavioral deterioration coupled with the consumption of diets rich in fat.

1. Introduction

Obesity is stemming from a complex interaction between genetic and environmental causes, with diet representing a major contributing factor (Gao and Horvath, 2008). Obesity is associated with a plethora of comorbidities such as type-2 diabetes, cardiovascular diseases, osteoarthritis, cancers and cognitive disorders (Faith et al., 2011; Gariepy et al., 2010; Hotamisligil, 2006; Mannan et al., 2016). Excessive caloric intake not only causes metabolic dysfunction but also triggers chronic low-grade inflammation in peripheral organs including adipose tissue, liver, skeletal muscle and pancreas, and also in the central nervous system, where it is referred as neuroinflammation (Gregor and Hotamisligil, 2011; Thaler et al., 2012). Neuroinflammation in obesity is characterized by elevated pro-inflammatory markers and activation of

glial cells such as astrocytes and microglia (Baufeld et al., 2016; Cansell et al., 2021; De Souza et al., 2005; Le Thuc and Rovère, 2016; Salvi et al., 2022), and is found in the cortex, the amygdala and the hippocampus as well as in the hypothalamus, a brain structure that controls feeding behavior and energy homeostasis (Miller and Spencer, 2014). Consequently, it has been postulated that neuroinflammation contributes to both cognitive dysfunctions identified in obesity, especially memory deficits and anxiety (Jeon et al., 2012; Noronha et al., 2019), and to metabolic alterations and eating disorders (Duriez et al., 2021; Gorwood et al., 2016; Méquinion et al., 2017).

Numerous investigations have highlighted the propensity of high-fat diets to trigger neuroinflammation, with specific attention to the role of nutritional lipids in this process (Guillemot-Legris et al., 2016; Guillemot-Legris and Muccioli, 2017). However, the nature of nutritional lipids that are responsible of this response remains incompletely elucidated. Incubation of different saturated and unsaturated fatty acid mixes on astrocytes cultures has allowed to identify that saturated fatty acids (SFA) induce the production of the pro-inflammatory cytokines interleukin 6 (IL-6) and tumor necrosis factor alpha (TNF-α) (Gupta et al., 2012; Valdearcos et al., 2014). The role of dietary polyunsaturated fatty acids (PUFA), as determinants of neuroinflammation has been also raised. PUFA, classified as ω3, ω6 and ω9 based on the relative location of double bonds in the carbon chain, play opposite roles in health and inflammation, with ω3 showing preventive effects (Demers et al., 2020; Dighriri et al., 2022; Simopoulos, 2002). Interestingly, *in vitro* co-incubation of SFA with the ω3 PUFA docosahexaenoic acid on astrocytes prevents release of pro-inflammatory cytokines (Gupta et al., 2012). Globally, low ω3 PUFA consumption might confer a risk for anxiety and depression (Kalkman et al., 2021; Müller et al., 2015). Nevertheless, to the best of our knowledge, comprehensive investigations into the *in vivo* effects of various high-fat diets, characterized by distinct compositions of SFA and PUFA, notably differing ω6/ω3 ratios, on neuroinflammation and cognitive function are lacking.

Here, we determined the effect of different natural diets rich in fat and with various ω6/ω3 ratios on energy metabolism and neuroinflammation. We show that a HFD with low ω6/ω3 ratio partly mitigates the deleterious effects of HFD on body weight gain and glucose metabolism and protects from chronic inflammation. Mice fed either medium or high ω6/ω3 ratio displayed classical phenotypes associated with HFD such as impaired glucose and insulin intolerance, elevated fasting glucose and insulin, but only high ω6/ω3 ratio was associated with neuroinflammation and the impairment of behavior. Our findings suggest that consumption of certain types of fatty acids may mitigate the behavioral effects associated with diet-induced obesity.

2. Material and methods

2.1. Animals and diets

Eight-week-old C57Bl/6J male mice (Janvier Labs, France) were housed in a room maintained at thermoneutrality (Fischer et al., 2019) (28 ± 2 °C) with an inversed 12-h light/dark cycle (lights off at 8 A.M.). Animals were housed in groups of 10 (Fig. S1) and each group fed for 12 or 20 weeks with either standard diet (CHOW; Standard Rodent Diet A03; SAFE, Augy, France) or HFD enriched in different natural sources of fat to modulate their ω6/ω3 ratios. HFD are low (2.9; HFD-LO; U8959 v20; SAFE, Augy, France), medium (7.3; HFD-ME; U8954 v100; SAFE, Augy, France) or high (21.1; HFD-HI; U8954 v216; SAFE, Augy, France) ω6/ω3 ratio. Female mice were only used to have a weight curve for 20 weeks. Macronutrient and fatty acids composition of each diet were analyzed by high performance liquid chromatography (HPLC and data are shown in Table S1. Animals had free access to water and food, which is changed every two days to avoid lipid peroxidation and palatability decrease (Nguemeni et al., 2010). In each group of 10 mice, 7 of them were euthanized under isoflurane for the collection of different tissues (Fig. S1) and blood and 3 of them were euthanized by intra-aortic

perfusion of 4 % paraformaldehyde for brain collection. All the protocols were carried out in accordance with French ethical guidelines for laboratory animals and with approval of the Animal Care Committee (Nice-French Riviera, project agreement APAFIS#25319-2020042317135371v2 and APAFIS#25320-2020042718555028v2).

2.2. Red blood cell and triglycerides isolation for lipid quantification

Total lipids from red blood cells were extracted using the method of Moilanen and Nikkari (Moilanen and Nikkari, 1981). Total lipids were then transmethylated with Boron trifluoride in methanol (Morrison and Smith, 1964). Hexane was used to extract fatty acid methyl esters (FAMEs) and dimethyl acetals (DMAs). The relative composition of FAMEs and DMAs was performed on a GC Trace 1310 (Thermo Scientific, Illkirch, France) gas chromatograph (GC) using a CPSIL-88 column (Agilent, CA, USA) and hydrogen as the vector gas as previously described (Bizeau et al., 2022). The GC device was coupled to a flame ionization detector (FID). Comparisons with commercial and synthetic standards enabled the identification of FAMEs and DMAs. The Chrom-Quest 5.0 version 3.2.1 software (Thermo Scientific, Illkirch, France) was used to process the data.

For triglycerides analysis, lipids from mouse serum were extracted according to a modified protocol (Bligh and Dyer, 1959) with a mixture of methanol/chloroform (2:1). The lipid extract was then separated on a C18 column in an appropriate gradient. Mass spectrometry data were acquired with a Q-exactive mass spectrometer (ThermoFisher, France) operating in data-dependent MS/MS mode (dd-MS2). Finally, lipids were identified using LipidSearch software v4.1.16 (ThermoFisher) in product search mode.

2.3. Metabolic cages for respirometry analysis

Promethion CAB-16 Cages (Promethion, Sable System International, USA) were used to house animals and assess respirometry analysis, energy expenditure, locomotor activity and food intake. Animals were acclimated in the cages during two days and all the parameters listed before were then measured during two days. A 16-channel Promethion system was used. Individual cages included a ceiling-mounted food hopper (3-mg resolution) and water spigot. Cages included a ceiling-mounted small "hut" into which mice could climb, which permits body mass measurements. X- and Y-axis (horizontal plane) photoelectric beam motion detectors were positioned around the cage. A running wheel accessory was available but was excluded from the current study. Airflow through the chamber was negative (2,000 mL/min), and gas analyses were recorded once per minute. Cages were mounted inside of thermally controlled cabinets that were maintained at thermoneutrality (30 °C) to match parameters utilized in the OxyMax system.

2.4. RNA isolation and quantitative PCR

Total mRNAs were isolated with the Chomczynski method (Chomczynski, 1987) using Fast Prep apparatus (Q-Biogene, France). Two micrograms of total mRNAs were denatured at 65 °C for 5 min in the presence of 0.5 mM dNTP and oligodT primers (25 ng/μl; Promega, France). Reverse transcription of mRNAs was performed using SuperScript III Reverse Transcriptase (100 U; Life Technologies, France) in a total volume of 20 μl. RT was diluted 5 times to be used in quantitative real-time PCR experiments (RT- qPCR). RT- qPCR was performed in a LightCycler 480 apparatus (Roche, France) using LightCycler 480 SYBR Green I Master (2x) as described by the manufacturer. Primers were designed using Primer Express 1.5 software (Applied Biosystems, USA) and are detailed in Table S2. Real-time PCR was performed for amplification of *Tnfa, Il1b, Il6, Ccl2, Ccl5, Aif1, Plin1, AdipoQ, Slc2a4, Gapdh* and *Tbp* mRNA. In each assay, PCR was performed in duplicate. Relative quantities of target genes were calculated with the ΔΔ CT method using *Gapdh* (for hypothalamus and hippocampus) or *Tbp* (for liver and

adipose tissues) as housekeeping genes.

2.5. Fluorescence in situ hybridization (FISH)

FISH was performed on fresh frozen brain sections (14 μm) with the RNAscope Multiplex Fluorescent Kit v2 in accordance to the manufacturer's protocol (Advanced Cell Diagnostics). Specific probes were used to detect *Aif1 (Allograft Inflammatory Factor 1)*, IBA1 coding gene (319141, NM_019467.2, target region 31–866), *Il6* (315891, NM_031168.1, target region 27–792) and *Il1b* (502431-C2, NM_008361.3, target region 2–950) mRNAs. Hybridization with a probe against the Bacillus subtilis dihydrodipicolinate reductase (*dapB*) gene (320871) was used as a negative control.

2.6. Immunohistochemistry experiments

Mice were perfused in intra-aortic with 4 % paraformaldehyde (PFA) and brains were collected. Immunostaining of IBA1 (microglia) and GFAP (astrocytes) was done on 30 μm thick brain floating sections. Immunostaining of Ki67 (proliferation marker) was done on same sections but a step of 10 min at 95 °C in Citrate buffer wad added prior to the staining. Rabbit anti-mouse IBA1 (1:300, #CP290A, Biocare Medical), GFAP (1:500, #Z0334, Dako), Rat anti-mouse Ki67 (1:300, #14–5698-82, Invitrogen) and Alexa 488 or Alexa 594 goat anti-rabbit secondary antibody (1:500, #A-11008 and #A-11012, Invitrogen) were used. Sections were mounted in Vectashield solution (H-1000, Vector Laboratories).

2.7. Fluorescence microscopy

Images mosaics for cell counting were acquired with an inverted epifluorescence microscope (Axiovert 200 M, Carl Zeiss, Rueil Malmaison, France) through a 10x/0,3 objective. Tri-dimensional high-resolution images for morphometric analysis of microglia were acquired with a Laser Scanning Confocal Microscope (TCS SP8, Leica, Microsystems, Nanterre, France) through a 63x/1.4 oil immersion objective with a voxel size of 70 x 70 x 500 nm.

2.8. Image analysis

Microglial cell counting was done with ImageJ / Fiji software (Schneider et al., 2012) on image mosaics of hypothalamus. After a background subtraction to filter somas, the cell number was obtained with "*Find maxima*" local maxima detection tool. Microglial morphology was characterized on hypothalamic tri-dimensional confocal z-stacks using Imaris® 9.6.1 software (Oxford Instruments, Belfast, UK). After a surface rendering on Iba1 staining to mask cells of interest, the morphological parameters were obtained through the *Filament tracer* tool. Morphological measurements of astrocytes was assessed using an activation score already described and commonly used (Cansell et al., 2021; Harrison et al., 2019).

2.9. Histological analysis

Dissected adipose tissues and liver were collected and weighed, fixed for 24 h in 4 % PFA, paraffin embedded, sliced into 10 μm thick sections using a microtome RM 2255 (Leica) and dried overnight at 37 °C. All sections were then deparaffinized in xylene, rehydrated through alcohol, and washed in phosphate-buffered saline. Hematoxylin-Eosin stained sections were imaged with the Vectra 3 slide scanner (Akoya Bisocences, USA) using a 10x/0.2 objective. The images were stored and managed on our University Côte d'Azur - EMBRC-Fr OMERO image database (Allan et al., 2012). Lipid droplet area measurement of each adipocyte of these images was performed using a home-made ImageJ /Fiji macro-program. This analysis was carried out on all the dataset containing the different images from diets in OMERO through the batch OMERO plugin (Pouchin et al., 2022).

2.10. Glucose tolerance test and insulin tolerance test

Glucose Tolerance Test (GTT) and Insulin Tolerance Test (ITT) were performed according to the IMPReSS guidelines (International Mouse Phenotyping Resource of Standardized Screens). Mice were fasted overnight (GTT) or 6 h (ITT) and placed into single cage housing for the duration of the test. Mice were left 1 h for habituation before basal glycemia values were established by measuring it in blood of tail vein using a glucose meter (Bayer Contour® XT) and test strips (Contour® Next). Glucose (1.5 g/kg body weight, Sigma-Aldrich) or human insulin (0.5 U/kg, Humalog, Lilly) diluted in NaCl 0.9 % was injected intra-peritoneal (ip) and blood glucose was measured again 15, 30, 45, 60, 90 and 120 min ip post-injection.

2.11. ELISA immunoassay

For plasma protein measurements, blood was collected by *retro-orbital* puncture, kept on ice and then centrifuged at 10,000 rpm for 10 min at 4 °C. Plasma was stored at −80 °C until further use. Pancreatic insulin content was obtained in accordance to "Pancreatic Insulin Content by Acid-Ethanol Extraction" protocol available on AMDCC Protocols (diacomp.org). Mouse ELISA kits were used for Insulin (ALPCO, USA), Leptin (AssayPro, USA), Adiponectin (AssayPro, USA), LBP (LPS binding protein, HycultBiotech, Netherlands) and Corticosterone (LDN, Germany) according to the manufacturer's protocols. IL-6 was measured with a V-Plex multiplex assay (MSD, USA) according to the manufacturer's protocols. Circulating level of lipopolysaccharide (LPS) was measured, as described in (Weil et al., 2019), by HPLC coupled with mass spectrometry using the 3-hydroxymyristate (3-HM) which is a lipid component of LPS.

2.12. Tomography analysis

Adipose tissue quantification was carried out using a SkyScan1178 X-ray micro-CT system. Mice were anesthetized and scanned using the same parameters: 104 m of voxel size, 49 kV, 0.5 mm thick aluminum filter, 0.9° of rotation step. Vertebrae size and total adipose tissue volume was measured between caudal vertebra 1 (C1) and thoracic vertebra 13 (T13) whereas subcutaneous (scWAT) and intra-abdominal (iaWAT) white adipose tissue surface were measured on one section between the lumbar 5 (L5) and the lumbar 6 (L6) level. ScWAT and iaWAT is based on the delimitation of region of interest after 3D reconstruction of scanned images as described in Reference 35. 3-D reconstructions and analysis of bone parameters and adipose tissue areas or volumes were performed using NRecon and CTAn software (Skyscan).

2.13. Behavioral tests

All the trials were video recorded and tracked using ANYmaze software (Stoelting Europe, Ireland).

2.13.1. Open field

Open field test was performed using a white and opaque quadratic arena (40x40cm) with an imaginary central area (20x20cm). The mouse was placed in the center of the arena and allowed to explore for 10 min. Number of entries and time spent in the imaginary central area were measured.

2.13.2. Dark light

Dark light test was done in white and black cage separated in two compartments. Mice were placed in the center of the dark compartment and allowed to explore for 5 min. Number of entries and time spent in the light compartment and latency to first exit the dark compartment were measured.

2.13.3. Morris water maze

Morris water maze test was done in a circular tank (Ø 90 cm) filled with water (temperature 25 ± 1 °C) made opaque with the addition of white opacifier (Viewpoint, France). The test consisted in 3 phases: Cue task (1 day), Spatial learning (4 days) and Memory probe test (1 day). An escape platform (Ø 8 cm) was submerged 1 cm below the water surface for the cue task and the spatial learning.

Cue task was done prior to spatial learning to detect visual and motor problems and to accustom the mice to the testing rule (find the platform to escape). A visible flag was placed on top of the platform and the maze was surrounded by opaque curtains. The mice were allowed to find the visible platform. The escape latency and average speed were recorded. For the spatial learning, the extra-maze cues were mounted on the sidewalls. A new platform position was chosen and kept in the same position for the four training days. If the animal did not find the platform within the trial duration it was gently guided to it. For the cue task and spatial learning, all animals performed four trials per day with a maximum trial duration of 90 s (+30 s on the platform at the end of each trial) and an inter-trial interval of 10 min. Twenty-four hours after training completion, the platform was removed, and a probe test was run for 60 s. During the probe test, the distance travelled in each quadrant (target (previous position of the platform), left, right and opposite) and the number of crosses in the previous platform localization were measured.

2.13.4. Zero maze

Zero maze test was run in a white circular runway (55 cm diameter, ring shaped) raised 60 cm from the floor. The corridor width is 5 cm and is divided into two open quadrants (open zone) facing two enclosed quadrants (close zone) with a 15 cm high wall. Mice were placed in an open zone facing a closed zone and allowed to explore for 5 min. Number of entries and time spent in open zones were measured.

2.14. Locomotor activity

An actimeter was used to assess locomotor activity in a novel cage over a period of 3 days (divided into 30 min periods). The measure obtained is a sum of forward, backward and stands up movements. The apparatus employed (Imetronic Apparatus, Pessac, France) consists of an individual novel cage (30 cm × 14 cm × 12 cm) attached to a continuous recording system that detects the horizontal movements of the animals using an infrared photocell system.

2.15. Correlation analysis

Non-parametric correlations, Spearman's rank correlation (ρ) (Spearman, 1987), were calculated between metabolic/inflammatory parameters measured after 20 weeks of dieting and fatty acids found in red blood cell membranes in pairwise fashion ($n_{tests} = 924$). We chose to only represent correlation for main fatty acids represented in red blood cells membrane: alpha-linolenic acid (ALA), linoleic acid (LA), arachidonic acid (AA), eicosapentaenoic acid (EPA) and docosahexaenoic acid (DHA). P-values were corrected for multiple testing using the false discovery rate (FDR) (Benjamini and Hochberg, 1995) and correlations with an FDR below 0.05 were considered statistically significant. The same procedure was applied to correlations between metabolic/inflammatory parameters and fatty acids found in circulating triglycerides ($n_{tests} = 1302$). In the correlation matrix, the colors correspond to the correlation coefficient (blue: negative correlation, red: positive correlation) and the size of the circles represent the strength of the correlation relationship (between −1 and 1). The largest circles represent the strongest interactions between two data sets.

Broader categories of fatty acids: SFA, unsaturated (UFA), monounsaturated (MUFA), PUFA, ω6, and ω3, were used for comparing the makeup of the diet to the measured levels of fatty acids in both red blood cells membranes and circulating triglycerides after 12 or 20 weeks of diet. Similar to the approach mentioned above, pairwise Spearman's rank correlations were calculated by comparing diet to red blood cells membranes ($n_{tests} = 36$) as well as diet to circulating triglycerides ($n_{tests} = 36$). This was repeated using ratios of certain relevant measurements: ω6/ω3, LA/ALA, and EPA/AA rather than fatty acid categories ($n_{tests} = 9$).

2.16. Statistical analysis

Normality of the data was checked using a Kolmorgorov-Smirnov test (with Dallal–Wilkinson–Lillie for p value). The ROUT method (robust regression and outlier removal) was used to identify outliers with a Q coefficient equal to 1 %. Variance equality was tested using an F-test. If samples fulfilled normal distribution and variance equality criteria, comparisons between groups were carried out using an unpaired *t* test for single comparison. If samples did not follow a normal distribution or had different variances, comparisons between groups were carried out using a nonparametric Mann–Whitney *U* test for a single comparison. Multiple comparisons were carried out using One-Way ANOVA if samples fulfilled normal distribution and Kruskal-Wallis if not. Multiple comparison was done using a Two-Way ANOVA for curve graphs (body weight, cumulative food intake, glucose and insulin tolerance test, locomotor activity and Morris water maze). A p-value lower than 0.05 was considered statistically significant. All tests were performed using GraphPad Prism 9.3.0. Numbers of animals used for each measurement are indicated in the figure legends.

3. Results

3.1. Dietary ω6/ω3 ratio modulate weight gain and adipose tissue hypertrophia

Mice were fed for 12 or 20 weeks with a HFD containing low (HFD-LO, 2.9), medium (HFD-ME, 7.3) or high ω6/ω3 ratio (HFD-HI, 21.1) (Fig. S1). Diet composition is detailed in Table S1. We verified, by performing correlation study, that fatty acids composition and ratios are reflected in circulating triglycerides (Fig. 1A) (short term incorporation, (Schneeman et al., 1993)) and red blood cells membrane (Fig. 1B) (long term incorporation, (Mu et al., 2006)) after 20 weeks of diet. We obtained the same results after 12 weeks of diet (Fig. S2). Compared to the standard diet, all diets induced weight gain but starting at various times; from week 9 for HFD-HI, week 11 for HFD-ME and 13 for HFD-LO (Fig. 1C) and only for male mice since no difference in weight gain was measured for females across the groups (Fig. S3). At 20 weeks, body weight was not different between HFD-ME and HFD-HI (Fig. 1C). Cumulative calories intake of HFD-LO mice was not different from the control group, while HFD-ME and HFD-HI showed the same increased food intake (Fig. 1D), suggesting that higher body weight in HFD-LO is caused by a decrease in energy expenditure, rather than an increase in energy intake. To test for differences in energy expenditure, we subjected mice under the different dietary regimen to indirect respirometry and assessed locomotor activity. Unexpectedly, the respiratory exchange ratio as well as energy expenditure, daily food intake and locomotor activity were similar across groups (Fig. 1E-H). Compared to the other HFD groups, HFD-LO mice showed very moderate differences in tissue morphology such as less hypertrophy and no change in liver weight at both 12 and 20 weeks (Table 1).

To strengthen the evaluation of ω6/ω3 ratio on adipose tissue function, Plin1, AdipoQ, Slc2a4 (coding for GLUT4) gene expression were measured in scWAT and pgWAT (Fig. S4A-F). In accordance with hypertrophia measured in Table 1, we showed an increased expression of gene coding for Perilipin in scWAT and Adiponectin in pgWAT. Levels of mRNA encoding Glut4 seem much more affected in pgWAT, which is the tissue that plays a role in physiology, notably in glucose transport and insulin response. At the hormonal level, fasting adiponectin levels were not modified in both HFD while leptin levels were elevated in HFD-
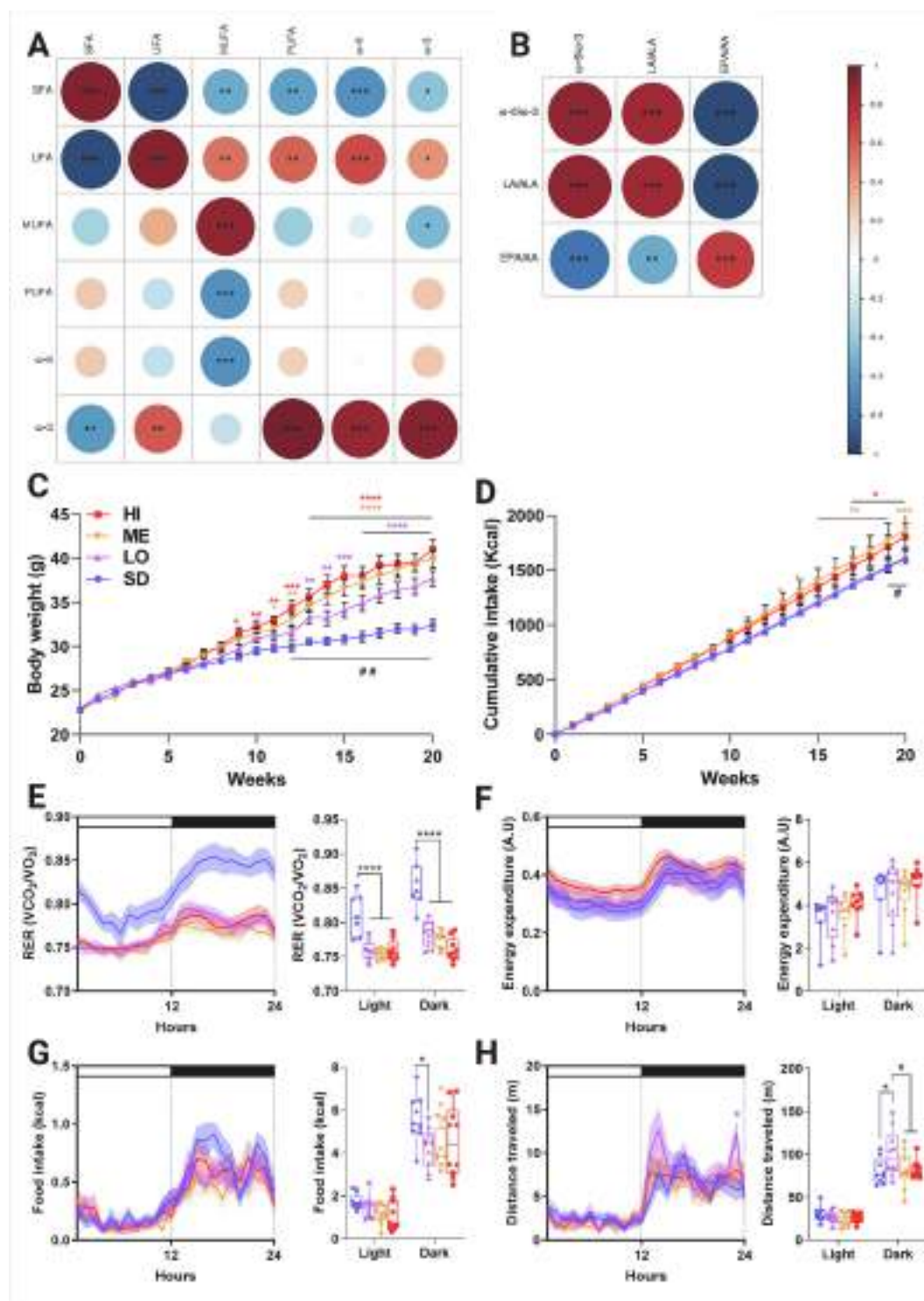
Fig. 1. Lipids in diets are found back in circulating triglycerides and red blood cell membrane and low ω6/ω3 ratio attenuates weight gain and food intake after 20 weeks of diet. (A) Correlation study between fatty acids in diets (rows) and inside circulating triglycerides (columns). (B) Correlation study between fatty acids ratios in diets (rows) and in red blood cells membrane (columns). Colors are corresponding to the correlation coefficient (blue: negative correlation, red: positive correlation) and sizes of the circles represent the strength of the correlation relationship (between −1 and 1). (C) Body weight during 20 weeks of diets (SD or HFD-LO/HFD-ME/HFD-HI); n = 20 per diet. (D) Cumulative intake in kilocalories during 20 weeks of diets; n = 20 per diet. Metabolic cages analysis after 20 weeks of diet with (E) daily variation in the RER and corresponding AUC; n = 10 per diet, (F) daily variation in energy expenditure and corresponding AUC; n = 10 per diet, (G) daily variation in food intake and corresponding AUC; n = 10 per diet and (H) daily variation in locomotor activity and corresponding AUC; n = 10 per diet. Values obtained in male mice are expressed as mean ± SEM; *p ≤ 0.05, **p ≤ 0.01, ***p ≤ 0.001, ****p ≤ 0.0001, *compared to SD. #p ≤ 0.05, ##p ≤ 0.01, HFD-LO compared to HFD-HI.

Table 1

Low ω6/ω3 ratio attenuates adipose tissue and liver hypertrophia and lipid storage inside those tissues. (Upper table) Data represents tissue weight (mg) of subcutaneous white adipose tissue (scWAT), perigonadal white adipose tissue (pgWAT), brown adipose tissue (BAT) and liver, adipocytes area (μm^2) for the scWAT, pgWAT and BAT and lipid droplet area (μm^2) in liver after 12 or 20 weeks of diet. Values obtained in male mice are expressed as mean $\pm$ SEM; *p $\leq$ 0.05, **p $\leq$ 0.01, ***p $\leq$ 0.001, ****p $\leq$ 0.0001, *compared to SD.

		12 weeks			
		SD	HFD-LO	HFD-ME	HFD-HI
Tissue weight (mg)	scWAT	251.9 ± 20.05	383.3 ± 35.39	549.3 ± 24.67 **	369.1 ± 23.79
	pgWAT	314.9 ± 65.06	431.2 ± 93.2	686.6 ± 113.4 **	507.4 ± 109.6 *
	isBAT	113.4 ± 23.42	114.99 ± 16.18	119.5 ± 21.9	110.7 ± 21.38
	Liver	414.0 ± 23.55	434.16 ± 53.88	560.89 ± 59.57 **	429.18 ± 48.27
Adipocytes area (μm^2)	scWAT	821.4 ± 24.62	1131 ± 76.21 *	1270 ± 62.74 **	1107 ± 97.81 *
	pgWAT	611.5 ± 39.77	642.4 ± 39.94	1491 ± 70.95 ***	1118 ± 119.5 **
	isBAT	104.8 ± 5.504	94.02 ± 4.449	127.6 ± 9.048 *	116.4 ± 4.794
Lipid droplet area (μm^2)	Liver	nd	nd	41.81 ± 3.189	nd

		20 weeks			
		SD	HFD-LO	HFD-ME	HFD-HI
Tissue weight (mg)	scWAT	271.7 ± 44.07	567.2 ± 71.09 *	827.3 ± 104.6 ***	618.1 ± 97.73**
	pgWAT	347.8 ± 76.31	690.0 ± 27.32 ***	792.5 ± 52.96 ****	531.0 ± 34.76 **
	isBAT	121.2 ± 13.28	110.2 ± 16.12	203.0 ± 14.14 **	156.7 ± 19.22
	Liver	450.0 ± 20.84	577.0 ± 68.16	820.3 ± 10.66 *	695.5 ± 68.96
Adipocytes area (μm^2)	scWAT	903.8 ± 33.02	1136 ± 87.30	1940 ± 116.1 **	2074 ± 167.1 **
	pgWAT	611.4 ± 26.68	1452 ± 68.63 ****	1478 ± 69.69 ****	1587 ± 93.94 ****
	isBAT	120.2 ± 10.04	86.22 ± 2.802	164.9 ± 16.19 **	136.9 ± 13.29 *
Lipid droplet area (μm^2)	Liver	nd	55.90 ± 2.068	81.86 ± 1.071	54.94 ± 3.865

ME and HI, but not in LO (Fig. S4G-H). We also showed here that only HFD-ME and HI display a significantly reduced adiponectin/leptin ratio, considered as a marker of adipose tissue dysfunction (Frühbeck et al., 2018). Finally, tomography-based quantification of adipose tissue mass showed that HFD-LO mice have less adipose tissue volume and a prominent distribution into subcutaneous adipose tissue (Fig. S5). Our findings indicate that ω6/ω3 ratio play a role in programming adipose tissue hypertrophia and body weight notably by modulating food intake.

3.2. Dietary ω6/ω3 ratio drive distinct impaired glucose metabolism phenotypes

We next studied the impact of fatty acid composition on glucose metabolism and circulating leptin levels. While after 12 weeks into the different diets, glucose tolerance was not affected (Fig. 2A), after 20 weeks, glucose tolerance appeared to be slightly affected by HFD-HI after 20 weeks (Fig. 2B). Insulin tolerance was not impaired in the HFD-LO group while it was markedly affected in other HFD groups at 20 weeks (Fig. 2C-D). Fasting blood glucose levels were similarly elevated in mice fed under HFD (Fig. 2E). Interestingly, fasting insulin levels (Fig. 2F) and pancreatic insulin levels (Fig. 2G) were only elevated in HFD-HI. Together, these results suggest different etiologies of impaired glucose metabolism across the 3 HFD diets suggesting that different ω6/

ω3 ratios impair glucose metabolism through distinct mechanisms.

3.3. High ω6/ω3 is linked to higher expression of pro-inflammatory cytokines

Obesity is associated with various levels of chronic inflammation in peripheral tissues that is thought to play a role in the etiology of associated disorders (Hotamisligil, 2006). To evaluate the degree of inflammation in metabolic tissues, we measured the gene expression of pro-inflammatory cytokines in liver and in different adipose tissue depots. After 12 weeks of diet, the expression of *Tnfa* and *Il1b* was higher in the HFD-ME compared to other groups, while *Il6* was only higher in the HFD-HI group (Fig. 3A). Strikingly, at 20 weeks, all tested cytokines were only higher in the HFD-HI group (Fig. 3B). The expression of inflammatory cytokines was largely unaffected by diet in all high fat diets and adipose tissue depots, except for perigonadal fat at 20 weeks, where *Tnfa* and *Il6* expression was only higher in HFD-HI and *Il1b* was higher in the HFD-ME and HFD-HI groups (Fig. 3C-H). Moreover, we measured an increased circulating level of IL-6 for HFD-HI fed mice, which is known to be the major cytokine secreted in obesity (Eder et al., 2009), from 12 weeks of diet (Fig. S5A-B). We also measured an increased circulating level of LPS and LBP in HFD-HI fed mice after 20 weeks of diet (Fig. S5C-D). Collectively, these results suggest ω6/ω3 ratio drive chronic inflammation in blood, liver and adipose tissue despite similar impairment in glucose tolerance.

Given the differences that we detected in food intake and inflammation across diets on the one hand and the documented role of central inflammation on food intake in obesity on the other (Marcos et al., 2023), we next tested the association between ω6/ω3 intake and the expression of pro-inflammatory cytokines in the hypothalamus. Interestingly, we only detected higher expression of *Il1b*, *Il6* for the HFD-HI diet at 12 weeks and of *Il1b*, *Il6*, *Ccl2* and *Ccl5* after 20 weeks (Fig. 4A-B). Chemokines, especially CCL2/CCL5, are known activators of microglial cells, which exert immune functions in the brain (Skuljec et al. 2011; Selenica et al. 2013). To determine the activation level of microglial cells in the hypothalamus, we measured *Aif1* expression (coding for IBA1) by RT-qPCR. Compared to other diets, we detected a higher expression of mRNA encoding for IBA1 at 12 weeks for HFD-ME and HFD-HI and at 20 weeks for HFD-HI only (Fig. 4C-D). Thus, these results indicate that inflammation is triggered by HFD-HI in metabolic tissues and in the hypothalamus.

3.4. Dietary ω6/ω3 ratio influence microglial activation in hypothalamus

We next aimed to determine the effect of fatty acid composition on microglia activation. We quantified microglial number and cell ramifications by microscopy. While after 12 weeks, HFD-HI was only associated with increase in the total length of extensions and number of IBA1 positive cells (corresponding to microglial cells) in arcuate nucleus (ARC) (Fig. 5A-B), at 20 weeks, HFD-HI was associated with alteration in all parameters measured (Fig. 5C-D). This ramified microglial phenotype is also associated with more production of pro-inflammatory mRNA of *Il1b* and *Il6* (Fig. 5E-F). Interestingly, HFD-LO was associated with a lower amount of microglial extensions compared to controls (Fig. 5C-D). Further, we quantified that the increased number of IBA1 positive cells after 20 weeks of diet in ARC was coming from a proliferation mechanism as they are co-stained with Ki67 (Fig. S7). These results suggest that high ω6/ω3 ratio triggers microglial activation in the ARC.

3.5. High dietary ω6/ω3 ratio leads to a pro-inflammatory profile without microglial activation in hippocampus

Obesity is associated with psychological and cognitive disorders like anxiety, memory deficits and, depression (Singh, 2014). At 20 weeks, levels of inflammatory cytokines were higher in HFD-HI compared to other groups while mRNA encoding for IBA1 were not different (Fig. 6A-
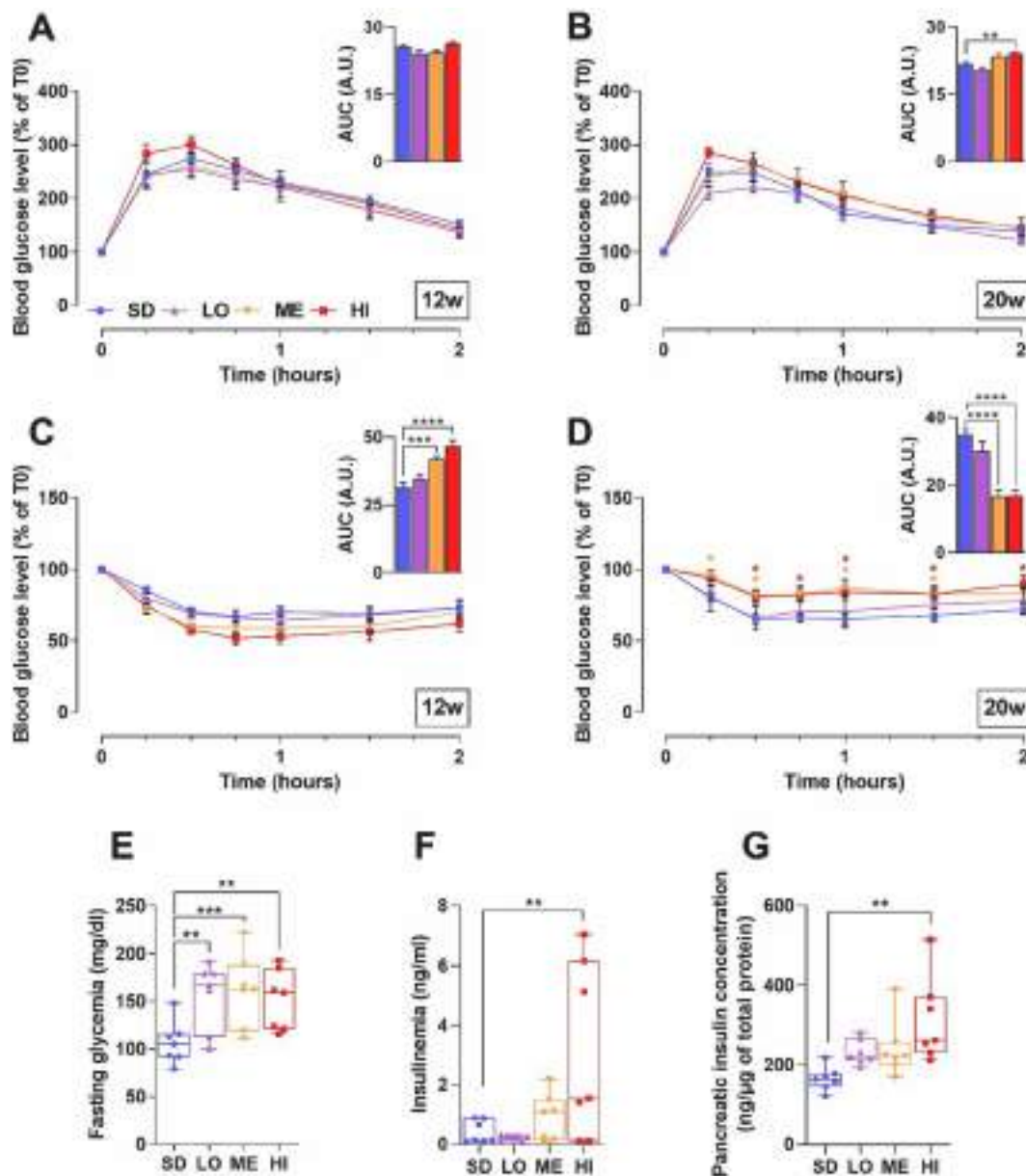
Fig. 2. Low ω6/ω3 ratio alleviates glucose metabolism disruption and avoid hyperinsulinemia/ hyperleptinemia. (A) Blood glucose curve following IP-GTT (Intraperitoneal Glucose Tolerance Test) at 12 weeks of diet; n = 10 per diet. (B) Blood glucose curve following IP-GTT at 20 weeks of diet; n = 10 per diet. (C) Blood glucose curve following IP-ITT (Intraperitoneal Insulin Tolerance Test) at 12 weeks of diet; n = 10 per diet. (D) Blood glucose curve following IP-ITT at 20 weeks of diet; n = 10 per diet. (E) Basal glycemia after 20 weeks of diet; n = 10 per diet. (F) Insulinemia, (G) pancreatic insulin concentration after 20 weeks of diet; n = 7 per diet. Values obtained in male mice are expressed as mean ± SEM; *p ≤ 0.05, **p ≤ 0.01, ***p ≤ 0.001, ****p ≤ 0.0001, *compared to SD.

B) in hippocampus, a brain region implicated in anxiety and memory (Engin and Treit, 2007; Voss et al., 2017). In the hippocampus, all features of microglial ramifications were comparable between all groups (Fig. 6C-D). However, we detected differences in astrocytes activation in hippocampus (Fig. S8) that could explain the higher level of inflammatory cytokines. Thus, a diet with high ω6/ω3 ratio induces an inflammatory state in the hippocampus coupled with an astrocyte activation.

3.6. High dietary ω6/ω3 ratio causes anxiety-like phenotype and spatial memory deficits

We first aimed to get insight into stress levels by measuring circulating levels of corticosterone. At 20 weeks, corticosterone levels were higher in HFD-HI compared to other groups (Fig. 7A). To determine if

hippocampal inflammation is associated with altered behavior, we performed three anxiety tests: Open Field (OF), Zero Maze (ZM) and Dark/Light Box (DLB). As all apparatus are under strong light, the center of OF, the open part of ZM and the light box of DLB are considered as an *anxious zone*. After 20 weeks, when obesity is established, HFD-HI fed mice spent less time in each respective anxious zone compared to other groups (Fig. 7B-D). Assessment of locomotor activity showed that only HFD-HI fed mice exhibit a hyperactivity pattern (Fig. 7E-F). Most interestingly, hyperactivity was only detected during the acclimatization period only, reflecting anxiety behavior associated with a novel environment. Collectively, these results show that high ω6/ω3 ratio elicits an anxiety-like phenotype in mice.

Given that hippocampus is also the control center of memory (Voss et al., 2017), and that obesity is associated with memory deficits in human (Lentoor, 2022), we performed a Morris-Water Maze to evaluate
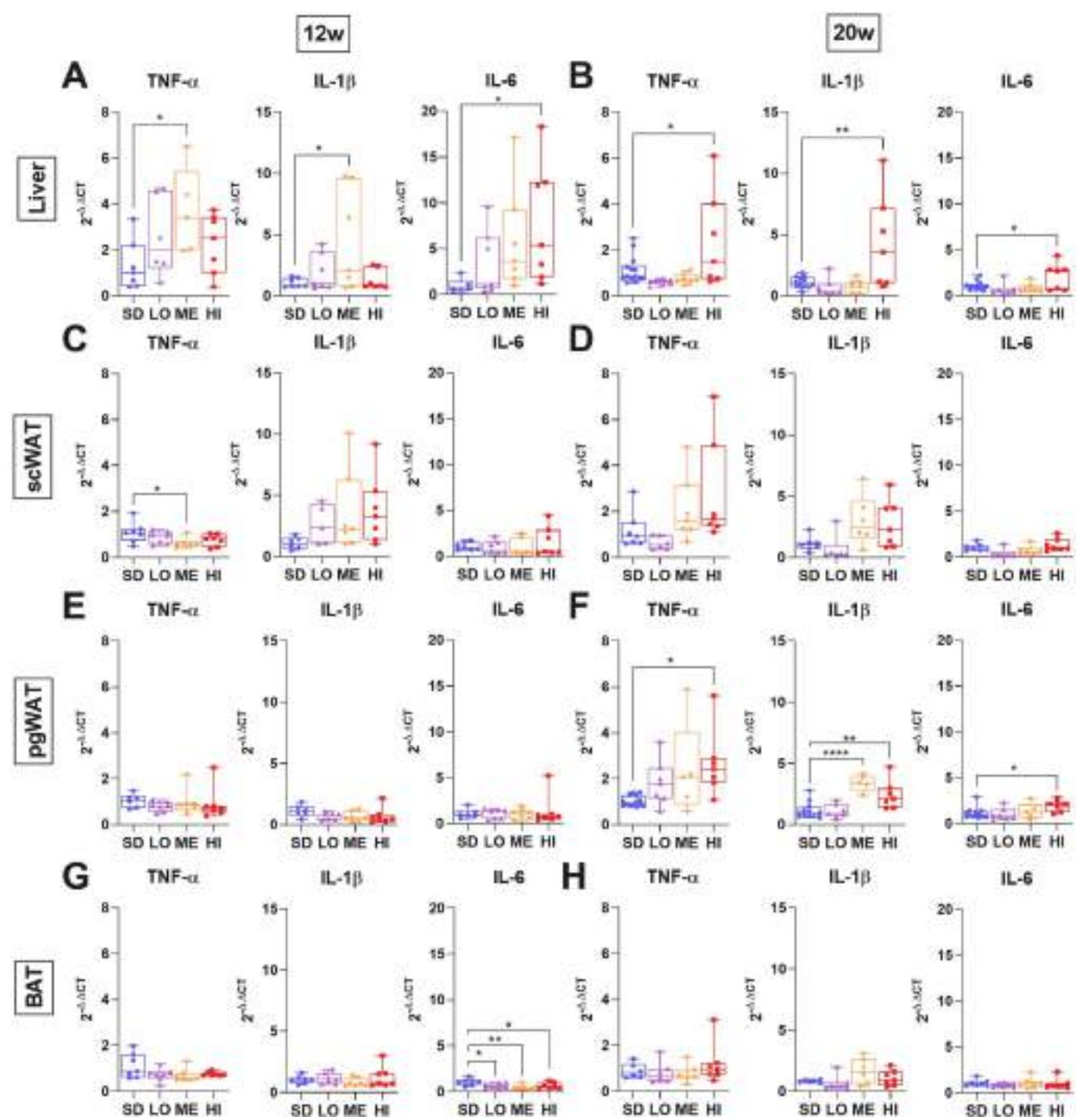
Fig. 3. High ω6/ω3 ratio triggers overexpression of pro-inflammatory cytokines in liver and perigonadal white adipose tissue. Quantification of mRNA encoding for pro-inflammatory cytokines: tumor necrosis factor alpha (TNF-α), interleukin-1 beta (IL-1β) and interleukin-6 (IL-6) (A) in liver after 12 weeks or (B) 20 weeks of diet, (C) in scWAT after 12 weeks or (D) 20 weeks of diet, (E) in pgWAT after 12 weeks or (F) 20 weeks of diet, (G) in BAT after 12 weeks or (H) 20 weeks of diet; n = 7 per diet. Values obtained in male mice are expressed as mean ± SEM; *p ≤ 0.05, **p ≤ 0.01, ****p ≤ 0.0001, *compared to SD.

spatial memory. We confirmed that mice did not have visual deficits using the cue task and checked no impairment in motor control through the measurement of swimming speed (Fig. 7G-H). Learning capacity was not altered, as the latency is decreasing in the same manner for all diets during the four days of training. However, HFD-HI fed mice displayed increased latency to reach the platform during the last trial of day 1, further indicating an anxiety-related behavior. Compared to other groups, only HFD-HI fed mice showed impaired spatial memory, with lower time spent searching the T quadrant and lower counts of crossing

events in a previous location (Fig. 7I-J). Furthermore, we measured that anxiety and memory deficits were not present before the onset of obesity after only 4 weeks of diet (Fig. S9). Collectively, these results show that fatty acid composition alters anxiety-related behavior and spatial memory and suggest that a high ω6/ω3 ratio is a determining factor.
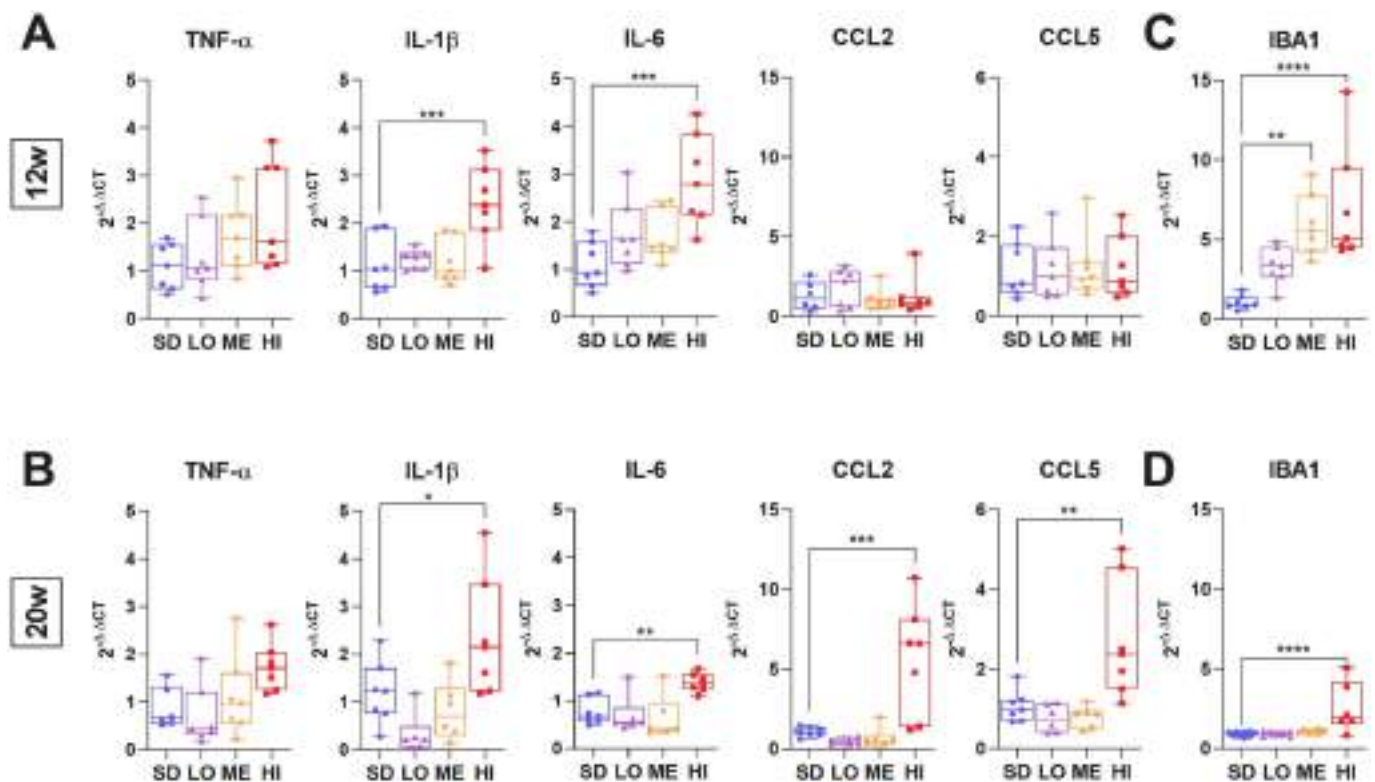
Fig. 4. High ω6/ω3 ratio induces overexpression of pro-inflammatory cytokines/chemokines and microglial activation marker in hypothalamus. Quantification of mRNA encoding for pro-inflammatory cytokines: TNF-α, IL-1β, IL-6 and chemokines CCL2 and CCL5 after (A) 12 weeks or (B) 20 weeks of diet. Quantification of mRNA encoding microglial activation marker IBA1 after (C) 12 weeks or (D) 20 weeks of diet; n = 7 per diet. Values obtained in male mice are expressed as mean ± SEM; *p ≤ 0.05, **p ≤ 0.01, ***p ≤ 0.001, ****p ≤ 0.0001, *compared to SD.

3.7. The proportion of ω3 and ω6 in red blood cell membranes correlates with both developments of obesity and inflammation

We used a multiple correlation approach to further investigate the impact of dietary fatty acids in the development of obesity and inflammatory parameters. Using the incorporation of dietary fatty acids into red blood cells membranes as a parameter reflecting the long-term impact of diet on animals (Mu et al., 2006), we first performed Spearman correlations between key PUFA and various metabolic variables (Fig. 8A) after 20 weeks of diet. Our results show that the enrichment of red cell membranes in ω3 is negatively correlated with the improved metabolic parameters, while enrichment in ω6 is positively associated. In particular, increased ω3 ALA, EPA and DHA in red cell membranes is associated with lower animal body weight and adipose tissue hypertrophy (Fig. 8A). Furthermore, ω3 DHA enrichment is also associated with lower blood leptin levels and adipocyte size in white adipose tissue. We found correlations between ω6 and metabolic parameters to be heterogeneous, since the correlation for LA with metabolic parameters was largely negative, but positive for AA. Enrichment in ω6 AA is associated with an increase in the weight of the various tissues collected.

We also analyzed the impact of long-term diets on peripheral and central inflammatory data. The correlation data strongly support a role for PUFA on peripheral inflammation and neuroinflammation (Fig. 8B). Most markedly, we observed that ω3 enrichment of red cell membranes is negatively correlated with gene expression levels of the pro-inflammatory markers *Tnfa, Il1b, Ccl2* and *Ccl5* in the hypothalamus and *Il1b, Il6* levels in the hippocampus. Only the microglia marker in the hypothalamus appeared to correlate negatively with ω3 enrichment, but the correlations were not statistically significant. On the other hand, the astrocyte marker does not seem to correlate for either the hypothalamus or the hippocampus. In peripheral tissues, ALA, EPA and DHA

enrichment levels are negatively correlated with *Tnfa, Il1b* and *Il6* levels in scWAT and *peri*-gonadal white adipose tissue (pgWAT), but no correlations were found for brown adipose tissue (BAT) and liver. Concerning ω6, and similar to the correlations with metabolic parameters (Fig. 8A), LA levels were not correlated with any of the inflammatory parameters studied.

In contrast, AA levels are positively correlated with *Tnfa* expression in hypothalamus and scWAT and *Il1b* expression in scwAT and pgWAT. We observed no significant correlation between ω6 enrichment of red cell membranes and the expression of inflammatory mediators in the hippocampus, BAT and liver. All the correlation data between PUFA in the red cell membrane and metabolic and inflammatory data are recapitulated in a summary chord diagram (Fig. S10). Thus, our analysis highlights a strong association between dietary intake of fatty acids and the metabolic or inflammatory phenotype.

4. Discussion

In this study, we investigated the effect of high fat diets with various dietary ω6/ω3 ratios on body weight gain, glucose metabolism, behavior and neuroinflammation in male mice. While all high fat diets induced weight gain, diets with high ω6/ω3 ratio were associated with more anxiety and impaired spatial memory, as well as increased neuroinflammation in the hypothalamus and hippocampus. Our study identified that the deleterious effect of diet induced obesity on body weight and energy metabolism are uncoupled with neuroinflammation.

Several strategies can be designed to study the metabolic and cognitive impact of different ω6/ω3 fatty acid ratios during chronic consumption of high-fat diets. A daily oral supplementation is efficient to provide defined quantities of fatty acids. However, this pharmacological approach requires repeated restraint of animals and gavage that generate stress, which can interfere with the direct behavioral and
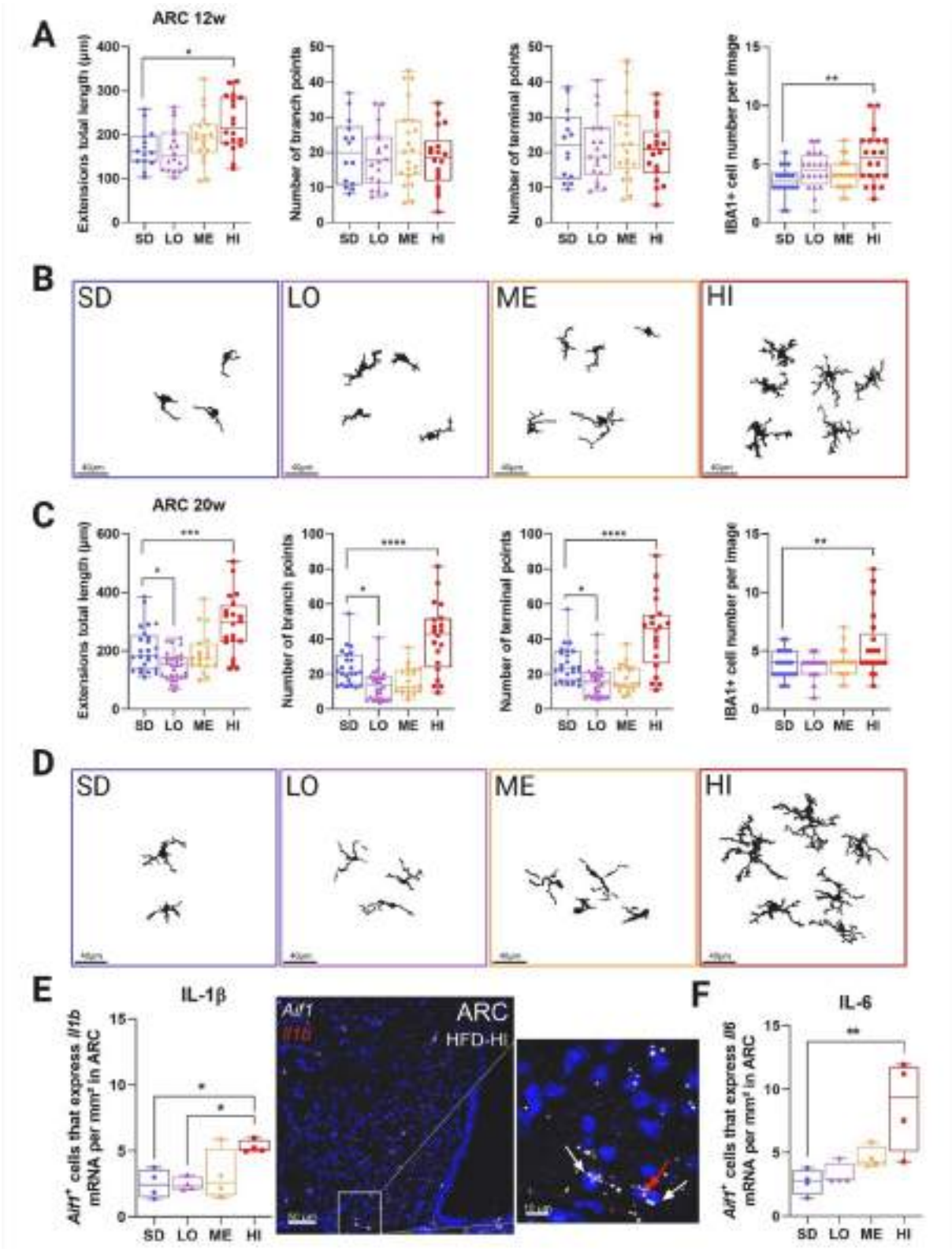
Fig. 5. High ω6/ω3 ratio drives ramification of microglia in hypothalamus. (A) Measure of microglia ramification in ARC with four parameters: Extensions total length (μm), number of branch points, number of terminal points and number of microglia in each image in ARC after 12 weeks of diet and (B) corresponding highlighted microglia on Imaris Software after immunohistochemical detection of IBA1 in ARC. (C) Measure of microglia ramification in ARC after 20 weeks of diet and (D) corresponding highlighted microglia object on Imaris Software after immunohistochemical detection of IBA1 in ARC; n = 7 per diet. (E) Number of Aif1 + cells expressing mRNA encoding for IL-1β per mm^2 in ARC and representative confocal image of fluorescence in situ hybridization experiments for Aif1 and Il1b mRNA after 20 weeks of diet. (F) Number of Aif1 + cells expressing mRNA encoding for IL-6 per mm^2 in ARC after 20 weeks of diet. Values obtained in male mice are expressed as mean ± SEM; *p ≤ 0.05, **p ≤ 0.01, ***p ≤ 0.001, ****p ≤ 0.0001, *compared to SD.

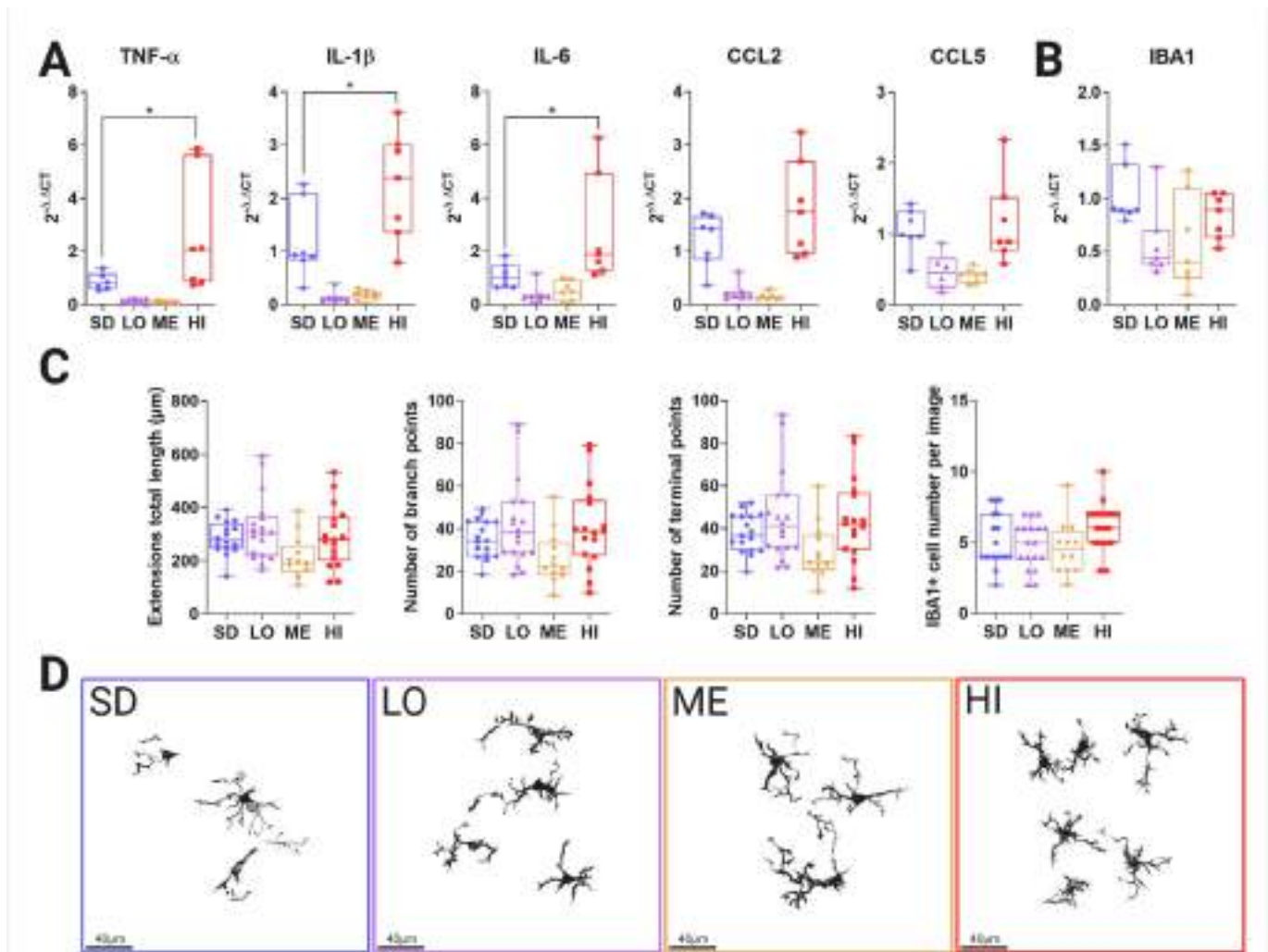**Fig. 6.** High ω6/ω3 ratio elicits overexpression of pro-inflammatory cytokines/chemokines in hippocampus without microglial activation and ramification. (A) Quantification of mRNA encoding for pro-inflammatory cytokines: TNF-α, IL-1β, IL-6 and chemokines CCL2 and CCL5, n = 7 per diet. (B) Quantification of mRNA encoding microglial activation marker IBA1, n = 7 per diet. (C) Measure of microglia ramification in CA3 with four parameters: Extensions total length (μm), number of branch points, number of terminal points and number of IBA1 positive cell in each image and (D) highlighted microglia on Imaris software after immunohistochemical detection of IBA1 protein, n = 3 per diet. All parameters are measured after 20 weeks of diet. Values obtained in male mice are expressed as mean ± SEM; *p ≤ 0.05, **p ≤ 0.01, *compared to SD.

cognitive effects from the high fat diets. Here, we opted for experimental diets enriched with vegetal oils given *ad libitum*. This unrestrained approach based on lipid-enriched diets in freely roaming animals limits stress and ensures the outcome of the behavioral testing. In addition, *ad libitum* feeding led to large inter-individual differences in total energy intake due to social interactions, specific feeding behavior and individual preferences, leading to differences in absolute amounts of ω6 and ω3 fatty acids within the same group. This heterogeneity has been revealed by biochemical assays and increased the power of the correlation study.

We designed natural diets with similar fat percentage while changing ω6/ω3 fatty acid ratio. Consequently, diets exhibited various saturated and unsaturated fat amounts. Thus, some of the metabolic, behavioral and cognitive effects induced during chronic consumption of the diets may have been, at least in part, triggered by SFA and not by ω6 or ω3 PUFA. Indeed, excess dietary SFA has been implicated in impaired cognition, memory and anxiety/depression like phenotype in the mouse (Dutheil et al., 2016; Greenwood and Winocur, 1990; Pistell et al., 2010). Since the total amount of SFA was similar between HFD-ME and HFD-HI (Table S1), our finding that only HFD-HI induced neuroinflammation and cognitive deficits suggests that saturated lipids may

not drive these effects. This is corroborated by our correlation analysis, which did not reveal strong association between saturated lipids and brain changes.

Supplementation in ω3 is associated with a lower risk to develop a plethora of diseases like cardiometabolic and neurodegenerative diseases (Dutheil et al., 2016; Marcelino de Andrade et al., 2017). By design, our diet with different ω6 and ω3 ratio lead to altering different PUFA independently; as both ω6 and ω3 are transformed and metabolized by the same enzymes, a relative dietary excess of one type of PUFA impairs the biosynthesis of the metabolites of the PUFA counterpart (Dyall et al., 2022). Yet, it is still possible that the pathophysiological consequences of the long-term HFD that we observed are directly due to variation in the absolute ω6 or ω3 amounts rather than secondary changes in the ω6/ω3 ratio. While the absolute amounts of ω3 totally differed in HFD-LO and HFD-HI (11.96 g/kg and 1.89 g/kg, respectively), the absolute amounts of ω6 were quite similar (34.41 g/kg and 40.03 g/kg) (Table S1). Thus, the increased ω3 amount alone might have provided a relative protection in the HFD-LO regimen.

Mice fed with HFD-LO exhibit an improved metabolic profile compared to HFD-ME and HFD-HI, with less weight gain associated with a lower cumulative food intake over 20 weeks. Compared to SD-fed
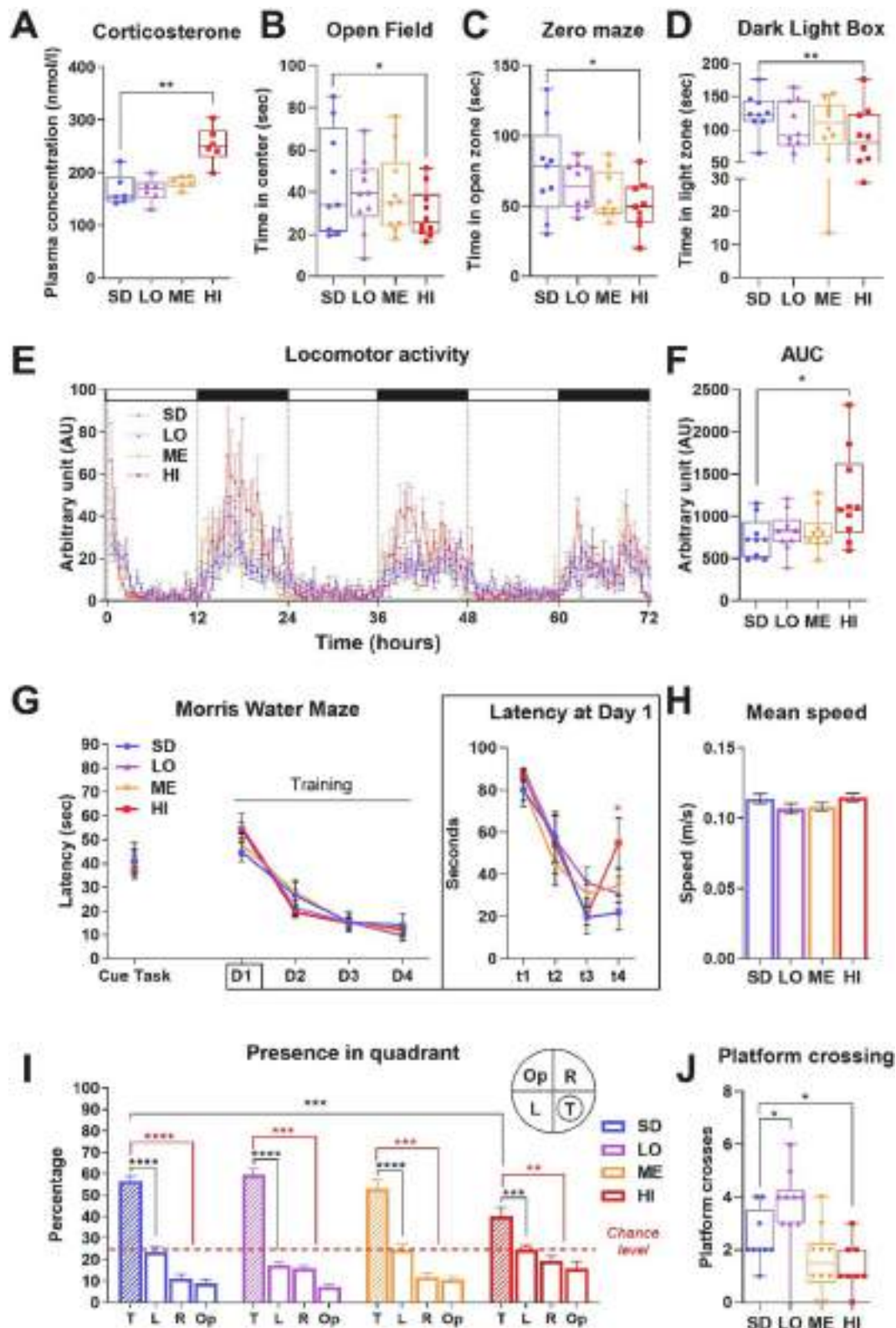
Fig. 7. High ω6/ω3 ratio causes higher circulating corticosterone associated with anxiety-like phenotype and spatial memory deficits. (A) Level of serum corticosterone (nmol/l), n = 7 per diet. (B) Time in center of open field. (C) Time in open zone of zero maze. (D) Time in light zone of dark/light box and latency to first exit from dark to light zone. (E) Locomotor activity and (F) corresponding AUC. (G) Data presented for cue task and learning represent average latencies to find the platform of four trials per day per mice. Data for latency at day 1 represent mean of all mice in a diet for each trial. (H) Mean speed of mice in the Morris water maze. (I) Percentage of presence in quadrant during probe test at 24 h after learning completion (T: Target, L: Left, R: Right, Op: Opposite). The persistence in the target quadrant is compared to chance level (considered at 25 %; red line). (J) Measure of the number of crosses in the previous platform localization. Values obtained in male mice are expressed as mean ± SEM; *p ≤ 0.05, **p ≤ 0.01, ***p ≤ 0.001, ****p ≤ 0.0001, *compared to SD.
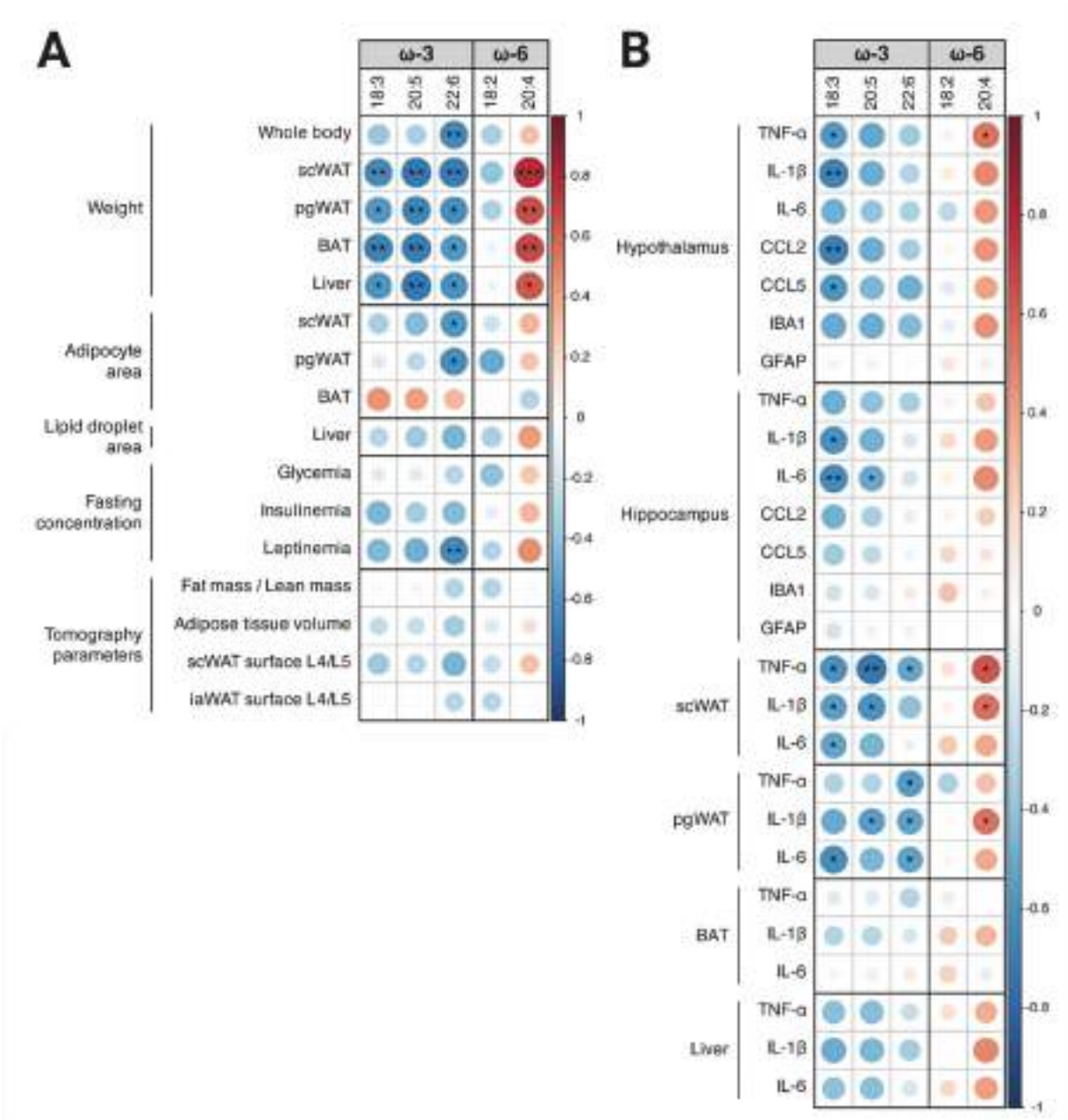
Fig. 8. Spearman correlation matrix between PUFA in red cell membrane and (A) metabolic parameters or (B) peripheral and central inflammatory parameters obtained in male mice after 20 weeks of diet. The PUFA used are ALA (18:3), EPA (20:5) DHA (22:6), LA (18:2) and AA (20:4). The values and colors (blue: negative correlation, red: positive correlation) in the boxes correspond to the correlation coefficient, sizes of the circles represent the strength of the correlation relationship (between −1 and 1) and the significance is relative to the dispersion of the data around the correlation line *p < 0.05, **p < 0.01, ***p < 0.001, *proximity of the data with the correlation line.

mice, HFD-LO mice show the same cumulative food intake over 20 weeks but lower food intake in the dark phase of metabolic cages. This may be due to the greater sensitivity of the measurement in the metabolic cages compared to the average weight of food consumed in the cages for cumulative food intake. However, these results are in line with numerous studies showing that ω3 supplementation protects against diet-induced glucose intolerance and attenuates overeating (Demers et al., 2020), although anti-obesity effects are not always observed (Demers et al., 2020; Marcelino de Andrade et al., 2017; Neto et al., 2021). Here, reduced weight gain in HFD-LO male mice was accompanied by a lower hypertrophy of adipocytes in white adipose tissues and a lower lipid storage in liver and brown adipose tissue compared to the other groups. We also demonstrate a less impaired function of white

adipose tissue in HFD-LO fed mice, with the ratio adiponectin/leptin, which is considered as a marker of adipose tissue dysfunction (Frühbeck et al., 2018), less diminished than the two others HFD groups. This is consistent with a previous study showing that ω3 fatty acids limit hypertrophy of adipose tissues and reduce lipid storage (Raclot and Oudart, 1999), two metabolic effects that may stem from a preferential distribution of ingested energy towards oxidation to the detriment of storage (Raclot and Oudart, 1999). In addition, HFD-LO male mice exhibited improved energy balance, with lower food intake and higher physical activity compared with other HFD groups, which contributes to the overall better metabolic profile of the HFD-LO mice.

Importantly, the metabolic consequences of the long term HFD are sex-dependent, since no difference in weight gain was measured in all

females kept on HFD. It was already shown that females gain less weight than males in response to an HFD diet (Hong et al., 2009). The diet used in this previous study contained 35 % lipids. Our data suggest that an HFD diet composed with 20 % lipids only is not sufficient to promote weight gain in female mice. One proposed mechanism is that ovarian hormones in females may be responsible for better regulation of metabolism (Hong et al., 2009).

The ability of ω3 fatty acids supplementation to reduce, or even supress, cognitive impairment associated with obesity is still largely debated (Marcelino de Andrade et al., 2017; Neto et al., 2023). In our study, animals fed HFD-LO showed no inflammatory markers in peripheral tissues or in the brain, suggesting that ω3 fatty acids during chronic long term HFD is sufficient to prevent peripheral and central inflammation. Conversely, we observed that only HFD-HI mice exhibit spatial memory deficits and anxiety-like phenotype. This supports a deleterious role of high ω6/ω3 ratio on cognitive performance, rather than the absolute quantity of ω3 alone.

We also found that long-term consumption of HFD with high ω6/ω3 ratio induced microglial activation, proliferation and ramification of microglia together with production of pro-inflammatory mediators in the hypothalamus. Interestingly, despite hippocampal-dependent behavior deficit and high level of neuroinflammatory markers within the hippocampus, changes in microglial morphology were not found in this area. Indeed, none of the 3 HFD caused changes in microglial morphology in the hippocampus after 20 weeks. This result indicates differences of microglial responsiveness toward chronic HFD according to brain areas. Similarly, a recent study showed that HFD induces deregulated inflammatory signaling pathways in hippocampal microglia without exhibiting changes in cell morphology (Henn et al., 2023). However, other studies reported significant morphological changes of hippocampal microglial upon chronic HFD (Cope et al., 2018; Hao et al., 2016). Such discrepancy in the hippocampus seems not to be related to the nature of the diet. For instance, saturated fats do not appear to be critical in inducing morphological changes of the microglia in this area since morphological changes of hippocampal microglia were neither detected in our study with diets low in SFA, which are known to directly bind to microglia and induce their activation *via* TLR-4 (Wang et al., 2012), nor in the study of Henn and colleagues which used diet with high level of SFA from lard (Henn et al., 2023). A possible explanation is that the HFD-induced morphological changes in hippocampal microglia are difficult to appreciate, in view of the constitutive hyper-ramification of these cells (Fig. 5 and Fig. 6). Additional work, coupling higher morphological resolution and expression of inflammatory markers at the single cell level is warranted to disentangle the complex relationship between inflammatory ability and morphological plasticity of the microglia in the hippocampus.

We found hippocampal-dependent cognitive dysfunction in response to chronic HFD, in HFD-HI mice, while neuroanatomical investigations revealed no morphological alteration in hippocampal microglia. This raises the possibility that neuroinflammation in this area might be driven by others cell types rather than microglia. For instance, astrocytes are able to produce pro-inflammatory mediators after lipid-stimulation (Gupta et al., 2012). Astrocytes are involved in numerous brain functions (Jessen, 2004) including memory processes (Chen et al., 2023). Inflammatory astrocytes are associated with mild cognitive impairment and severe dementia (Chun et al., 2020; Santello et al., 2019). Here, we found reactive astrocytes only in HFD-HI mice. Thus, reactive astrocytes might play a role in the cognitive deficit. Further investigations are needed to elucidate the exact role of astrocytes in the onset of neuroinflammation and cognitive deficits in diet-induced obesity.

In our study, in addition to neuroinflammation, we have also shown an increased level of LPS and LBP, which are markers of endotoxemia, in the HFD-HI. Recent studies suggest that HFD-induced metabolic endotoxemia (as increased circulating level of LPS and LBP) can impact on neuroinflammation, notably via microglial activation (Ben Fradj et al., 2022; Erny et al., 2015) and that LPS might reach the blood

compartment more easily when dietary fats are consumed (Ben Fradj et al., 2022). Thus, neuroinflammation observed in our conditions could depend on circulating LPS and LBP. However, our data reveal that the ω6/ω3 ratio correlates very powerfully with neuroinflammation. Indeed, correlative statistical analysis demonstrates a very strong link between the ω6/ω3 ratio and neuroinflammation, suggesting a specificity of the effect of this ratio. In the HFD-HI group, LPS and LBP increased, but so did all the other plasma parameters measured (leptin, glucose, insulin, corticosterone, IL-6 …), which also highly increased. It is therefore possible that the increase in these factors exacerbates the effect of the ω6/ω3 ratio and acts in potential synergy on the effect of the ω6/ω3 ratio.

Using a multiple correlation approach, we were able to see whether an increase in a certain type of PUFA in red blood cell membranes was associated with an increase in the metabolic and inflammatory parameters measured. Incorporation of dietary PUFAs in red blood cell is representative of incorporation in many other body tissues such as muscle, liver, heart and TA (Abbott et al., 2012). However, PUFAs are not incorporated in the same way depending on tissue location. For example, LA and AA for ω6 and ALA, EPA and DHA for ω3 incorporate into the membrane of red blood cells, while in the brain, LA and ALA only minimally incorporate compared to the other 3 main PUFA (AA, EPA and DHA) (Abbott et al., 2012). It is therefore possible that the correlations that we found between LA, ALA and brain-related parameters are due to indirect effects through the periphery, rather than a change in membrane composition of brain resident cells.

We found that ω3 enrichment in red blood cells membranes (ALA, EPA and DHA) is associated with less hypertrophy of adipose tissue and liver. In our study, hypertrophy of these tissues is associated with increased lipid storage. Thus, the increase in ω3 could be at the origin of a protective mechanism against lipid storage in adipose tissue and liver. It could be hypothesized that ω3 enrichment in tissues subject to lipid storage prevents this storage by promoting the oxidation process of lipids supplied by the diet (Raclot and Oudart, 1999). Conversely, enrichment of red blood cells membranes with AA ω6 is associated with increased hypertrophy of adipose tissue and liver. While our correlation analysis does no infer on a causal relationship between increased lipid storage in adipose tissue and AA membrane enrichment, the fact that AA is a precursor of many pro-inflammatory derivatives and inflammation is an aggravating factor in adipose tissue dysfunction in the pathology of obesity (Gregor and Hotamisligil, 2011) strongly support a mechanism by which increase dietary intake of AA induces lipid storage in adipose tissue.

With regard to inflammatory data, our results show that enrichment of red cell membranes with ALA ω3 and AA ω6 correlates respectively with a decrease and an increase in the expression of inflammatory markers in the hypothalamus. However, these data should be treated with caution for ALA, given that the proportion of ALA enrichment in brain membranes is very low. AA is a fatty acid that is well incorporated into brain membranes, and our results suggest a link between AA and inflammation. This is consistent with the literature, as enrichment of the cell membranes with ω6 AA promotes inflammation, whereas enrichment with ω3 EPA and DHA is conversely an anti-inflammatory factor (Calder, 2011). These observations stem from the fact that pro- and anti-inflammatory eicosanoids are derived directly from these PUFA and not from LA and ALA. We also observe these results for inflammation in white adipose tissue (scWAT and pgWAT).

Currently, the World Health Organization (WHO) recommends a dietary intake with a ω6/ω3 ratio from 1/1 to 4/1 however, the dietary intake of most developed and developing countries exceeds 10/1 (Simopoulos, 2002). In the present study, we used 3 distinct ω6/ω3 ratios ranging from 2.3 to 21.3 (HFD-LO: 2.9, HFD-ME: 7.3 and HFD-HI: 21.1). We have shown that obesity and inflammation are not directly correlated, but are dependent of the nature of the fatty acids contained in the diet. An HFD with a ω6/ω3 ratio in line with WHO recommendations (∼5) attenuates the obesity phenotype observed in our model.

Conversely, for the same weight gain, only HFD, whose ratio is close to the values consumed in the human diet (~14), leads to neuro-inflammation and cognitive deficits in the long term. We also showed a branched, pro-inflammatory phenotype of microglia in the hypothalamus in response to HFD with the high ratio. Thus, it is possible that microglial reactivity triggered by the pro-inflammatory environment of the diet used is at the root of the neuroinflammation and cognitive deficits observed.

In conclusion, our results show that the nature of dietary fatty acids independently drives metabolic dysfunction and neuroinflammation in obesity. However, mechanisms underlying the ω6/ω3 ratio effects are still undefined. Future studies should be done to address whether the effects of the ratio on the diet-induced immunometabolic phenotype are indirect or direct. Remodeling of lipid content in plasma membrane in the periphery may constitute a mechanism by which distinct dietary ω6/ω3 ratios alter energy metabolism, mood and cognition. Our study provides evidence for designing dietary interventions based on low ω6/ω3 ratio to combat obesity and its associated neurological disorders.

Author contributions

C.S. and C.R. conceived and supervised the study and designed the experiments. C.S. performed the majority of the experiments, interpreted results and generated figures. C.C. collected preliminary data and participated in the extraction of red blood cells and tissues. N.G. performed and analyzed tomography experiments. J.S. performed LPS and LBP measurements. M.V. contributed to behavioral tests and results interpretation. L.F. performed triglycerides measurements. C.R. and N.B. designed the diets. C.S., C.R., A.B. and R.B. wrote and revised the manuscript. P.N., A.A., C.P. and P.S. performed the statistics and correlation analysis. F.B. assisted to imaging analysis. E.Z.A. and A.S. contributed to experiments design. J.L.N. revised the manuscript.

CRediT authorship contribution statement

Clara Sanchez: Writing – review & editing, Writing – original draft, Supervision, Software, Methodology, Investigation, Formal analysis, Data curation, Conceptualization. **Cécilia Colson:** Methodology, Investigation. **Nadine Gautier:** Methodology, Investigation. **Pascal Noser:** Formal analysis. **Juliette Salvi:** Methodology, Investigation, Formal analysis. **Maxime Villet:** Methodology, Investigation, Formal analysis. **Lucile Fleuriot:** Methodology, Investigation. **Caroline Peltier:** Formal analysis. **Pascal Schlich:** Formal analysis. **Frédéric Brau:** Software, Methodology. **Ariane Sharif:** Supervision, Methodology. **Ali Altintas:** Supervision, Formal analysis. **Ez-Zoubir Amri:** Writing – review & editing, Validation, Supervision. **Jean-Louis Nahon:** Resources. **Nicolas Blondeau:** Validation, Resources, Conceptualization. **Alexandre Benani:** Writing – review & editing, Writing – original draft, Supervision, Conceptualization. **Romain Barrès:** Writing – original draft, Supervision, Resources. **Carole Rovère:** Formal analysis.

Data availability

Data will be made available on request.

Appendix A. Supplementary data

Supplementary data to this article can be found online at https://doi.org/10.1016/j.bbi.2024.01.216.

References

Allan, C., Burel, J.-M., Moore, J., Blackburn, C., Linkert, M., Loynton, S., Macdonald, D., Moore, W.J., Neves, C., Patterson, A., Porter, M., Tarkowska, A., Loranger, B., Avondo, J., Lagerstedt, I., Lianas, L., Leo, S., Hands, K., Hay, R.T., Patwardhan, A., Best, C., Kleywegt, G.J., Zanetti, G., Swedlow, J.R., 2012. OMERO: flexible, model-driven data management for experimental biology. Nat. Methods 9, 245–253. https://doi.org/10.1038/nmeth.1896.

Baufeld, C., Osterloh, A., Prokop, S., Miller, K.R., Heppner, F.L., 2016. High-fat diet-induced brain region-specific phenotypic spectrum of CNS resident microglia. Acta Neuropathol. (berl.) 132, 361–375. https://doi.org/10.1007/s00401-016-1595-4.

Benjamini, Y., Hochberg, Y., 1995. Controlling the false discovery rate: a practical and powerful approach to multiple testing. J. r. Stat. Soc. Ser. B Methodol. 57, 289–300. https://doi.org/10.1111/j.2517-6161.1995.tb02031.x.

Bizeau, J.-B., Albouery, M., Grégoire, S., Buteau, B., Martine, L., Crépin, M., Bron, A.M., Berdeaux, O., Acar, N., Chassaing, B., Bringer, M.-A., 2022. Dietary inulin supplementation affects specific plasmalogen species in the brain. Nutrients 14, 3097. https://doi.org/10.3390/nu14153097.

Bligh, E.G., Dyer, W.J., 1959. A rapid method of total lipid extraction and purification. Can. J. Biochem. Physiol. 37, 911–917. https://doi.org/10.1139/o59-099.

Calder, P.C., 2011. Fatty acids and inflammation: The cutting edge between food and pharma. Eur. J. Pharmacol. 668, S50–S58. https://doi.org/10.1016/j.ejphar.2011.05.085.

Cansell, C., Stobbe, K., Sanchez, C., Le Thuc, O., Mosser, C., Ben-Fradj, S., Leredde, J., Lebeaupin, C., Debayle, D., Fleuriot, L., Brau, F., Devaux, N., Benani, A., Audinat, E., Blondeau, N., Nahon, J., Rovère, C., 2021. Dietary fat exacerbates postprandial hypothalamic inflammation involving glial fibrillary acidic protein-positive cells and microglia in male mice. Glia 69, 42–60. https://doi.org/10.1002/glia.23882.

Chen, Y.-H., Jin, S.-Y., Yang, J.-M., Gao, T.-M., 2023. The memory orchestra: contribution of astrocytes. Neurosci. Bull. 39, 409–424. https://doi.org/10.1007/s12264-023-01024-x.

Chomczynski, P., 1987. Single-Step Method of RNA Isolation by Acid Guanidinium Thiocyanate-Phenol-Chloroform Extraction 4.

Chun, H., Im, H., Kang, Y.J., Kim, Y., Shin, J.H., Won, W., Lim, J., Ju, Y., Park, Y.M., Kim, S., Lee, S.E., Lee, J., Woo, J., Hwang, Y., Cho, H., Jo, S., Park, J.-H., Kim, D., Kim, D.Y., Seo, J.-S., Gwag, B.J., Kim, Y.S., Park, K.D., Kaang, B.-K., Cho, H., Ryu, H., Lee, C.J., 2020. Severe reactive astrocytes precipitate pathological hallmarks of Alzheimer's disease via H2O2- production. Nat. Neurosci. 23, 1555–1566. https://doi.org/10.1038/s41593-020-00735-y.

Cope, E.C., LaMarca, E.A., Monari, P.K., Olson, L.B., Martinez, S., Zych, A.D., Katchur, N. J., Gould, E., 2018. Microglia play an active role in obesity-associated cognitive decline. J. Neurosci. 38, 8889–8904. https://doi.org/10.1523/JNEUROSCI.0789-18.2018.

De Souza, C.T., Araujo, E.P., Bordin, S., Ashimine, R., Zollner, R.L., Boschero, A.C., Saad, M.J.A., Velloso, L.A., 2005. Consumption of a fat-rich diet activates a proinflammatory response and induces insulin resistance in the hypothalamus. Endocrinology 146, 4192–4199. https://doi.org/10.1210/en.2004-1520.

Demers, G., Roy, J., Machuca-Parra, A.I., Dashtehei pour, Z., Bairamian, D., Daneault, C., Rosiers, C.D., Ferreira, G., Alquier, T., Fulton, S., 2020. Fish oil supplementation alleviates metabolic and anxiodepressive effects of diet-induced obesity and associated changes in brain lipid composition in mice. Int. J. Obes. 44, 1936–1945. https://doi.org/10.1038/s41366-020-0623-6.

Dighriri, I.M., Alsubaie, A.M., Hakami, F.M., Hamithi, D.M., Alshekh, M.M., Khobrani, F. A., Dalak, F.E., Hakami, A.A., Alsueaadi, E.H., Alsaawi, L.S., Alshammari, S.F., Alqahtani, A.S., Alawi, I.A., Aljuaid, A.A., Tawhari, M.Q., 2022. Effects of omega-3 polyunsaturated fatty acids on brain functions: a systematic review. Cureus 14, e30091.

Duriez, P., Nilsson, I.A.K., Le Thuc, O., Alexandre, D., Chartrel, N., Rovere, C., Chauveau, C., Gorwood, P., Tolle, V., Viltart, O., 2021. Exploring the mechanisms of

recovery in anorexia nervosa through a translational approach: from original ecological measurements in human to brain tissue analyses in mice. Nutrients 13, 2786. https://doi.org/10.3390/nu13082786.

Dutheil, S., Ota, K.T., Wohleb, E.S., Rasmussen, K., Duman, R.S., 2016. High-fat diet induced anxiety and anhedonia: impact on brain homeostasis and inflammation. Neuropsychopharmacology 41, 1874–1887. https://doi.org/10.1038/npp.2015.357.

Dyall, S.C., Balas, L., Bazan, N.G., Brenna, J.T., Chiang, N., da Costa Souza, F., Dalli, J., Durand, T., Galano, J.-M., Lein, P.J., Serhan, C.N., Taha, A.Y., 2022. Polyunsaturated fatty acids and fatty acid-derived lipid mediators: recent advances in the understanding of their biosynthesis, structures, and functions. Prog. Lipid Res. 86, 101165 https://doi.org/10.1016/j.plipres.2022.101165.

Eder, K., Baffy, N., Falus, A., Fulop, A.K., 2009. The major inflammatory mediator interleukin-6 and obesity. Inflamm. Res Off. J. Eur. Histamine Res. Soc. Al 58, 727–736. https://doi.org/10.1007/s00011-009-0060-4.

Engin, E., Treit, D., 2007. The role of hippocampus in anxiety: intracerebral infusion studies. Behav. Pharmacol. 18, 365–374. https://doi.org/10.1097/FBP.0b013e3282de7929.

Faith, M.S., Butryn, M., Wadden, T.A., Fabricatore, A., Nguyen, A.M., Heymsfield, S.B., 2011. Evidence for prospective associations among depression and obesity in population-based studies: prospective obesity-depression associations. Obes. Rev. 12, e438–e453. https://doi.org/10.1111/j.1467-789X.2010.00843.x.

Fischer, A.W., Cannon, B., Nedergaard, J., 2019. The answer to the question "What is the best housing temperature to translate mouse experiments to humans?" is: thermoneutrality. Mol. Metab. 26, 1–3. https://doi.org/10.1016/j.molmet.2019.05.006.

Gao, Q., Horvath, T.L., 2008. Neuronal control of energy homeostasis. FEBS Lett. 582, 132–141. https://doi.org/10.1016/j.febslet.2007.11.063.

Gariepy, G., Nitka, D., Schmitz, N., 2010. The association between obesity and anxiety disorders in the population: a systematic review and meta-analysis. Int. J. Obes. 34, 407–419. https://doi.org/10.1038/ijo.2009.252.

Gorwood, P., Blanchet-Collet, C., Chartrel, N., Duclos, J., Dechelotte, P., Hanachi, M., Fetissov, S., Godart, N., Melchior, J.-C., Ramoz, N., Rovere-Jovene, C., Tolle, V., Viltart, O., Epelbaum, J., 2016. New insights in anorexia nervosa. Front. Neurosci. 10 https://doi.org/10.3389/fnins.2016.00256.

Greenwood, C.E., Winocur, G., 1990. Learning and memory impairment in rats fed a high saturated fat diet. Behav. Neural Biol. 53, 74–87. https://doi.org/10.1016/0163-1047(90)90831-p.

Gregor, M.F., Hotamisligil, G.S., 2011. Inflammatory mechanisms in obesity. Annu. Rev. Immunol. 29, 415–445. https://doi.org/10.1146/annurev-immunol-031210-101322.

Guillemot-Legris, O., Masquelier, J., Everard, A., Cani, P.D., Alhouayek, M., Muccioli, G. G., 2016. High-fat diet feeding differentially affects the development of inflammation in the central nervous system. J. Neuroinflammation 13, 206. https://doi.org/10.1186/s12974-016-0666-8.

Guillemot-Legris, O., Muccioli, G.G., 2017. Obesity-induced neuroinflammation: beyond the hypothalamus. Trends Neurosci. 40, 237–253. https://doi.org/10.1016/j.tins.2017.02.005.

Gupta, S., Knight, A.G., Gupta, S., Keller, J.N., Bruce-Keller, A.J., 2012. Saturated long-chain fatty acids activate inflammatory signaling in astrocytes. J. Neurochem. 120, 1060–1071. https://doi.org/10.1111/j.1471-4159.2012.07660.x.

Hao, S., Dey, A., Yu, X., Stranahan, A.M., 2016. Dietary obesity reversibly induces synaptic stripping by microglia and impairs hippocampal plasticity. Brain. Behav. Immun. 51, 230–239. https://doi.org/10.1016/j.bbi.2015.08.023.

Harrison, L., Pfuhlmann, K., Schriever, S.C., Pfluger, P.T., 2019. Profound weight loss induces reactive astrogliosis in the arcuate nucleus of obese mice. Mol. Metab. 24, 149–155. https://doi.org/10.1016/j.molmet.2019.03.009.

Henn, R.E., Guo, K., Elzinga, S.E., Noureldein, M.H., Mendelson, F.E., Hayes, J.M., Rigan, D.M., Savelieff, M.G., Hur, J., Feldman, E.L., 2023. Single-cell RNA sequencing identifies hippocampal microglial dysregulation in diet-induced obesity. iScience 26, 106164. https://doi.org/10.1016/j.isci.2023.106164.

Hong, J., Stubbins, R.E., Smith, R.R., Harvey, A.E., Núñez, N.P., 2009. Differential susceptibility to obesity between male, female and ovariectomized female mice. Nutr. J. 8, 11. https://doi.org/10.1186/1475-2891-8-11.

Hotamisligil, G.S., 2006. Inflammation and metabolic disorders. Nature 444, 860–867. https://doi.org/10.1038/nature05485.

Jeon, B.T., Jeong, E.A., Shin, H.J., Lee, Y., Lee, D.H., Kim, H.J., Kang, S.S., Cho, G.J., Choi, W.S., Roh, G.S., 2012. Resveratrol attenuates obesity-associated peripheral and central inflammation and improves memory deficit in mice fed a high-fat diet. Diabetes 61, 1444–1454. https://doi.org/10.2337/db11-1498.

Jessen, K.R., 2004. Glial cells. Int. J. Biochem. Cell Biol. 36, 1861–1867. https://doi.org/10.1016/j.biocel.2004.02.023.

Kalkman, H.O., Hersberger, M., Walitza, S., Berger, G.E., 2021. Disentangling the molecular mechanisms of the antidepressant activity of omega-3 polyunsaturated fatty acid: a comprehensive review of the literature. Int. J. Mol. Sci. 22, 4393. https://doi.org/10.3390/ijms22094393.

Le Thuc, O., Rovère, C., 2016. Inflammation hypothalamique et dérégulations de la balance énergétique : focus sur les chimiokines. Biol. Aujourdhui 210, 211–225. https://doi.org/10.1051/jbio/2016026.

Lentoor, A.G., 2022. Obesity and neurocognitive performance of memory, attention, and executive function. NeuroSci 3, 376–386. https://doi.org/10.3390/neurosci3030027.

Mannan, M., Mamun, A., Doi, S., Clavarino, A., 2016. Prospective associations between depression and obesity for adolescent males and females- a systematic review and meta-analysis of longitudinal studies. Plos One 11, e0157240.

Marcelino de Andrade, A., Fernandes, M. da C., de Fraga, L.S., Porawski, M., Giovenardi, M., Guedes, R.P., 2017. Omega-3 fatty acids revert high-fat diet-induced neuroinflammation but not recognition memory impairment in rats. Metab. Brain Dis. 32, 1871–1881. https://doi.org/10.1007/s11011-017-0080-7.

Marcos, J.L., Olivares-Barraza, R., Ceballo, K., Wastavino, M., Ortiz, V., Riquelme, J., Martínez-Pinto, J., Muñoz, P., Cruz, G., Sotomayor-Zárate, R., 2023. Obesogenic diet-induced neuroinflammation: a pathological link between hedonic and homeostatic control of food intake. Int. J. Mol. Sci. 24, 1468. https://doi.org/10.3390/ijms24021468.

Méquinion, M., Le Thuc, O., Zgheib, S., Alexandre, D., Chartrel, N., Rovère, C., Hardouin, P., Viltart, O., Chauveau, C., 2017. Long-term energy deficit in mice causes long-lasting hypothalamic alterations after recovery. Neuroendocrinology 105, 372–383. https://doi.org/10.1159/000455048.

Miller, A.A., Spencer, S.J., 2014. Obesity and neuroinflammation: a pathway to cognitive impairment. Brain. Behav. Immun. 42, 10–21. https://doi.org/10.1016/j.bbi.2014.04.001.

Moilanen, T., Nikkari, T., 1981. The effect of storage on the fatty acid composition of human serum. Clin. Chim. Acta Int. J. Clin. Chem. 114, 111–116. https://doi.org/10.1016/0009-8981(81)90235-7.

Morrison, W.R., Smith, L.M., 1964. Preparation of fatty acid methyl esters and dimethylacetals from lipids with boron fluoride–methanol. J. Lipid Res. 5, 600–608.

Mu, H., Thøgersen, R.L., Maaetoft-Udsen, K., Straarup, E.M., Frøkiaer, H., 2006. Different kinetic in incorporation and depletion of n-3 fatty acids in erythrocytes and leukocytes of mice. Lipids 41, 749–752. https://doi.org/10.1007/s11745-006-5026-5.

Müller, C.P., Reichel, M., Mühle, C., Rhein, C., Gulbins, E., Kornhuber, J., 2015. Brain membrane lipids in major depression and anxiety disorders. Biochim. Biophys. Acta 1851, 1052–1065. https://doi.org/10.1016/j.bbalip.2014.12.014.

Neto, J., Jantsch, J., de Oliveira, S., Braga, M.F., Castro, L.F. dos S., Diniz, B.F., Moreira, J.C.F., Giovenardi, M., Porawski, M., Guedes, R.P., 2021. DHA/EPA supplementation decreases anxiety-like behaviour, but it does not ameliorate metabolic profile in obese male rats. Br. J. Nutr. 1–11. https://doi.org/10.1017/S0007114521003998.

Neto, J., Jantsch, J., Rodrigues, F., Squizani, S., Eller, S., Oliveira, T.F., Silveira, A.K., Moreira, J.C.F., Giovenardi, M., Porawski, M., Guedes, R.P., 2023. Impact of cafeteria diet and n3 supplementation on the intestinal microbiota, fatty acids levels, neuroinflammatory markers and social memory in male rats. Physiol. Behav. 260, 114068 https://doi.org/10.1016/j.physbeh.2022.114068.

Noronha, S.S.R., Lima, P.M., Campos, G.S.V., Chírico, M.T.T., Abreu, A.R., Figueiredo, A. B., Silva, F.C.S., Chianca, D.A., Lowry, C.A., De Menezes, R.C.A., 2019. Association of high-fat diet with neuroinflammation, anxiety-like defensive behavioral responses, and altered thermoregulatory responses in male rats. Brain. Behav. Immun. 80, 500–511. https://doi.org/10.1016/j.bbi.2019.04.030.

Pistell, P.J., Morrison, C.D., Gupta, S., Knight, A.G., Keller, J.N., Ingram, D.K., Bruce-Keller, A.J., 2010. Cognitive impairment following high fat diet consumption is associated with brain inflammation. J. Neuroimmunol. 219, 25–32. https://doi.org/10.1016/j.jneuroim.2009.11.010.

Pouchin, P., Zoghlami, R., Valarcher, R., Delannoy, M., Carvalho, M., Belle, C., Mongy, M., Desset, S., Brau, F., 2022. Easing batch image processing from OMERO: a new toolbox for ImageJ. F1000Research 11, 392. https://doi.org/10.12688/f1000research.110385.2.

Raclot, T., Oudart, H., 1999. Selectivity of fatty acids on lipid metabolism and gene expression. Proc. Nutr. Soc. 58, 633–646. https://doi.org/10.1017/S002966519900083X.

Salvi, J., Andreoletti, P., Audinat, E., Balland, E., Ben Fradj, S., Cherkaoui-Malki, M., Heurtaux, T., Liénard, F., Nédélec, E., Rovère, C., Savary, S., Véjux, A., Trompier, D., Benani, A., 2022. Microgliosis: a double-edged sword in the control of food intake. FEBS J. febs.16583 https://doi.org/10.1111/febs.16583.

Santello, M., Toni, N., Volterra, A., 2019. Astrocyte function from information processing to cognition and cognitive impairment. Nat. Neurosci. 22, 154–166. https://doi.org/10.1038/s41593-018-0325-8.

Schneeman, B.O., Kotite, L., Todd, K.M., Havel, R.J., 1993. Relationships between the responses of triglyceride-rich lipoproteins in blood plasma containing apolipoproteins B-48 and B-100 to a fat-containing meal in normolipidemic humans. Proc. Natl. Acad. Sci. u. s. a. 90, 2069–2073. https://doi.org/10.1073/pnas.90.5.2069.

Schneider, C.A., Rasband, W.S., Eliceiri, K.W., 2012. NIH Image to ImageJ: 25 years of image analysis. Nat. Methods 9, 671–675. https://doi.org/10.1038/nmeth.2089.

Simopoulos, A.P., 2002. The importance of the ratio of omega-6/omega-3 essential fatty acids. Biomed. Pharmacother. 56, 365–379. https://doi.org/10.1016/S0753-3322(02)00253-6.

Singh, M., 2014. Mood, food, and obesity. Front. Psychol. 5 https://doi.org/10.3389/fpsyg.2014.00925.

Spearman, C., 1987. The proof and measurement of association between two things. Am. J. Psychol. 100, 441. https://doi.org/10.2307/1422689.

Thaler, J.P., Yi, C.-X., Schur, E.A., Guyenet, S.J., Hwang, B.H., Dietrich, M.O., Zhao, X., Sarruf, D.A., Izgur, V., Maravilla, K.R., Nguyen, H.T., Fischer, J.D., Matsen, M.E., Wisse, B.E., Morton, G.J., Horvath, T.L., Baskin, D.G., Tschöp, M.H., Schwartz, M.W., 2012. Obesity is associated with hypothalamic injury in rodents and humans. J. Clin. Invest. 122, 153–162. https://doi.org/10.1172/JCI59660.

Valdearcos, M., Robblee, M.M., Benjamin, D.I., Nomura, D.K., Xu, A.W., Koliwad, S.K., 2014. Microglia dictate the impact of saturated fat consumption on hypothalamic

inflammation and neuronal function. Cell Rep. 9, 2124–2138. https://doi.org/10.1016/j.celrep.2014.11.018.

Voss, J.L., Bridge, D.J., Cohen, N.J., Walker, J.A., 2017. A closer look at the hippocampus and memory. Trends Cogn. Sci. 21, 577–588. https://doi.org/10.1016/j.tics.2017.05.008.

Wang, Z., Liu, D., Wang, F., Liu, S., Zhao, S., Ling, E.-A., Hao, A., 2012. Saturated fatty acids activate microglia via Toll-like receptor 4/NF-κB signalling. Br. J. Nutr. 107, 229–241. https://doi.org/10.1017/S0007114511002868.